University of Nevada, Reno

CALPHAD Modeling of Phase Diagram Boundaries for Binary 2-Amino-2-Methyl-1,3-Propanediol [AMPL] and Tris(hydroxymethyl) Aminomethane [TRIS] system

A thesis submitted in partial fulfillment of the
Requirements for degree of Master of Science
in Materials Science and Engineering

by

Prathyusha Mekala

Dr. Dhanesh Chandra/Thesis Advisor

December, 2010

University of Nevada, Reno
Statewide • Worldwide

THE GRADUATE SCHOOL

We recommend that the thesis
prepared under our supervision by

PRATHYUSHA MEKALA

entitled

Calphad Modeling Of Phase Diagram Boundaries For Binary 2-Amino-2-Methyl-1,3 Propanediol [Ampl] And Tris(Hydroxymethyl)Aminomethane System.

be accepted in partial fulfillment of the
requirements for the degree of

MASTER OF SCIENCE

Dr. Dhanesh Chandra, Advisor

Dr. Wen-Ming Chien, Committee Member

Dr. Jaak Daemen, Graduate School Representative

Marsha H. Read, Ph. D., Associate Dean, Graduate School

December, 2010

Abstract

The phase diagram assessment of binary AMPL-TRIS system was calculated using the CALPHAD approach. Thermo-Calc, TCC software was used to fit the experimental phase diagram data by simultaneous optimization of thermodynamic properties of pure components and phase equilibria data available in the literature, and also calculated in the present work. The measured interaction parameters for low temperature α and β solid solution phases are relatively small and are assumed to be ideal. Preliminary calculation of AMPL-TRIS phase diagram showed complete solid solubility of the high temperature γ and γ' phases, as reported by Barrio et al. (1994). In the next iteration, we calculated AMPL-TRIS phase diagram using heat capacity data and found that it was in good agreement with the current experimental phase diagram developed by V. Kamisetty (2010). In final calculations, the Parrot module of Thermo-Calc program was used to obtain an optimized phase diagram. The calculated phase corroborates well with V. Kamisetty data. Two eutectoids, one at ~21 mol.% TRIS at 85^{o}C, the other at ~60 mol. % TRIS at 104^{o}C, and one peritectic at 55 mol.% TRIS at 127^{o}C were calculated. The maximum solubility of TRIS in AMPL is 10 mol.%, and that of AMPL in TRIS is 18 mol.% at 85^{o}C. An important feature of this phase diagram is the presence of γ and γ' phases above 110^{o}C. Details of the methodology and calculations are shown in this thesis.

Acknowledgements

I would like to express my immense gratitude to my advisor Prof. Dhanesh Chandra who pioneered me in to new area of research, also for his continuous encouragement throughout my M.S. I greatly acknowledge the financial, intellectual, and moral support that he has provided. Prof. Chandra has been a constant source of inspiration and he has spent countless hours working with me to bring my research to fruition.

I would like to thank Dr. Wen-Ming Chien, and Prof. Jaak Daemen for serving on my committee.

I would also like to acknowledge the help of UNR alumni Dr. Raja Chellappa for his wonderful guidance and patience in answering my questions. I greatly appreciate their time and patience.

I would express my gratitude Dr. Zi-kui-Liu and Paul Mason of Materials Genome in supplying the THERMO-CALC software and aiding in working with the software.

I also owe a huge debt of gratitude to my parents, my best friend in UNR Anasuya Adibhatla and my childhood friend Vasu for always being there when I have needed them.

Table of Contents

List of Tables

Chapter 2

Chapter 3

List of Figures

Chapter 2

CHAPTER 1

INTRODUCTION

1.1. Thermal Energy storage materials

The storage of thermal energy and its utilization are important roles in conservation of energy. The phenomenon involved in the energy storage is such that the heating and cooling cycles either absorb or emit heat at the transformation. In general, the energy storage is accomplished by either phase transformations of a material or by storing the heat as sensible heat in the lattice of a material. Phase Change Materials (PCMs) store heat by phase transitions and can be categorized in to two groups organic and inorganic. Organic PCMs have high gravimetric latent heat, low pressure, non-corrosive, chemically stable, little supercooling, low thermal conductivity, large changes in volume during phase change [1].

Depending on their applications PCMs are selected based on their melting points or solid state phase transition temperatures. PCMs are chosen in such a way that the thermal gradient between the storage temperature and the substance temperature should be kept minimum by use of PCMs' phase change temperatures. In one of the applications these materials are suggested for use in the making of concrete and brick. The use of PCMs for thermal storage in cooling and heating buildings was one of the first applications in the literature by Telkes in 1975 [2]. Materials that melt below 15 ^{o}C are used for cooling applications such as air conditioning, while materials that melt above 90 ^{o}C are used for

absorption refrigeration [1]. Apart from the latent heat, sensible heat is also stored by the PCMs making the overall efficiency of the system higher.

In general, PCMs may be classified as (1) solid- liquid, (2) gas-solid and (3) solid-solid phase change materials. The examples of solid-liquid PCMs are paraffins, salt hydrates and metals. The salt hydrates such as sodium sulfate deca-hydrate and calcium chloride hexa-hydrate [3-4] have large enthalpies of transformation near or below room temperature; sodium triacetate hydrate is an example of this material.

Metal hydrides store energy by transforming from solid to gas. The energy generated from the reaction of formation of metal hydride from pure metal is stored in the lattice of the material [5]. Substituted $LaNi_5 - xMx$, where M = Sn, Gd, Al, or excess Ni, is a potential candidate for this type of storage medium. Polyalcohols such as pentaerythritol, pentaglycerine, neopentylglycol, and amines exhibit crystalline transformations which absorb and emit large amounts of heat by phase transitions from solid to solid [6]. Latent heat is stored in the crystal and when a transition occurs, at a specific temperature, called the transition temperature (T_t), energy changes take place. Plastic crystals are good candidates for energy storage material because freedom of molecular rotation exists in the very crystalline state on account of their globular shape. After the melting point is reached, the coherence of the crystal is disrupted [7].

1.2. Solid-Solid PCMs

Solid-solid PCMs have been focused very little due to their smaller latent heat and higher phase change temperatures in low temperature heat-storage applications [8]. It was found

that polyalcohols (layered perovskites) and polyethylene are becoming the most important area of research. Among three the Polyalcohols are more efficient in low temperature energy storage applications. Besides the sensible heat polyalcohols also has additional solid-solid phase transformation energies in the range 20-80 cal/gm depending on the number of the O-H···O bonds. Polyalcohols exhibit tetragonal structures. An alloy mixture of different Polyalcohols in a molar ratio leads to the adjustment of its temperature, can be used in the application of interest.

Polyalcohols materials exhibit polymorphism on solid to solid phase transformation. Polyalcohols with functional group (CH_3, CH_2OH and NH_2) transform from low temperature heterogeneous α or β to high temperature cubic γ' or γ intermediate orientationally disordered crystal phases also called as 'Plastic Crystals'. These 'Plastic Crystals' store energy reversibly. The low temperature anisotropic phases α and β change to disordered isotropic high temperature phases absorbing a great deal of hydrogen bond energy at the solid-solid transition temperature. Few materials like 2- amino-2- methyl-1,2- propanediol (AMPL) [$(NH_2)C(CH_3)(CH_2OH)_2$], pentaerythritol [PE: $(CH_2OH)_2C(CH_2OH)_2$], neopentylglycol [NPG: $(CH_3)_2C(CH_2OH)_2$], neopentylalcohol [NPA: $(CH_3)_3C(CH_2OH)$], pentaglycerine [PG: $(CH_3)C(CH_2OH)_3$], and tris(hydroxymethyl) aminomethane [TRIS: $(NH_2)C(CH_2OH)_3$] are being investigated for their energy storage capabilities. Murrill and Breed (1970) have reported the transition parameters in the compounds $CR^1R^2R^3R^4$ where R^s are methyl, methylol, amino and carboxy groups. The solid-solid transition phenomenon can be observed in the temperature range 20 ^oC to 200

^{o}C, from ordinary to plastic crystals is acquired by a very high value of C_p before the transition point [9].

Dr. Chandra's group put efforts for a long period in investigating the thermodynamic data experimentally to study the organic solid-solid phase change thermal storage materials 'Plastic Crystals'.

1.3. An Overview on TRIS-AMPL Phase Diagram

Materials are subjected to high pressure and temperatures to study their affect on the phase transitions. By calculating the phase diagrams one can see through the phase stabilities of solid solutions over the temperature range of interest. Chandra et al. [10-11] have reported pure component heat capacities, enthalpy and transition temperatures for AMPL, TRIS, TRMP, PE, NPG etc.. Chellappa and Chandra [12-14] reported computer simulated phase diagrams for PE-PG, PE-NPG, PG-AMPL, NPG-AMPL, TRIS-AMPL, NPG- TRIS, PG-TRIS and PE-TRIS, using FACT/ Thermo-Calc programs using the heat capacity data and showed that there is an excellent correlation between the experimental phase diagram and computer generated ones.

We are currently working on TRIS-AMPL, TRMP-AMPL systems. In 1993 Barrio et al. [14] constructed experimental TRIS-AMPL phase diagram with the results of thermal analysis and crystallographic studies in the range of temperatures 25 ^{o}C to 177 ^{o}C [15]. Zhang et al, have measured the thermal conductivities of AMPL and TRIS individual systems and both as a binary system with 50:50 mixture [16]. Thermodynamic and crystallographic data for the system has been investigated by numerous researchers [3-

16]. The experimental phase diagram of AMPL-TRIS has been determined by Mr. Vamsi K. Kamisetty [21] and the experimental data will be used as a comparison of this calculated AMPL-TRIS phase diagram presented in this work. Thermodynamic data has been collected for calculating AMPL-TRIS phase diagrams of plastic crystal materials on the basis of the CALPHAD method. The heat capacity measurements of pure and solid solutions TRIS and AMPL are key input to computer modeling of binary phase diagrams using CALPHAD method.

1.4. CALPHAD

CALPHAD has been an efficient tool for the last 30 years in utilizing available experimental data and performing a thermodynamic optimization. Since the pioneering work by Kaufman who also derived the name CALPHAD, the CALPHAD modeling of thermodynamics has been developed into a sophisticated approach capable of calculating phase equilibria in multi-component, technologically important materials. The journal CALPHAD is started in 1977 under the editorship of Larry Kaufman. It not only has the assessed databases and optimized parameters for alloys but also has databases for oxides, salts, aqueous and organic systems comprising the major portion of the journal CALPHAD [16]. It also has many articles on application and the development of the different solution models to different material problems. The journal has been primary source of references for different kinds of thermodynamic assessments of alloy systems. The CALPHAD approach is particularly valuable in materials science and engineering in comparison with physics and chemistry due to more complicated systems involving multi component solution phases. The accuracy is achieved, if all the experimental data

available are taken into account and if thermodynamic consistency exists between every thermodynamic functions of the phases and the phase diagram.

We focused on optimization of the TRIS-AMPL binary phase diagram data from the experiments conducted by Chandra's research group, also in contributing to the development of the database with thermodynamic description of these PCMs. The Optimization and the development of the database were achieved through programming in computer software 'Thermo-Calc'. In a variety of applications like materials development to process control these self-consistent databases having complete thermodynamic descriptions of unary, binary, ternary and higher order systems are being used in equilibrium calculations. The assessed database contains the calculated Gibbs energies from the experimentally determined C_p data for individual phases as a function of temperature, composition and pressure. These databases are then linked to the Thermo-Calc for the computing the phase equilibria. The information should be stored in a compact form. The success of the model in correlating with the experimental phase diagram relies on the reliability of these databases.

There are three major problems associated with the generation of phase diagrams from experimental data, to which computer calculations are useful: the phase diagram should be as accurate as possible [17]. A powerful tool is necessary to evaluate the enormous number of unknown parameters of multi-component systems.

1.5. Thermo-Calc Software package

A number of software packages dealing with the equilibrium calculations for the databank development are available, e.g.: THERMO-CALC, Chemsage, Thermosuite, MTDATA, FACT, and Pandat. Thermo-Calc has been proved worldwide to be the most powerful and flexible tool based upon powerful Gibbs energy minimize, which can help in avoiding time consuming experiments, improve quality, performance and control environmental impacts. For the calculations of thermodynamic properties which can include functions with temperature, pressure, composition, magnetic ordering, chemical potential, etc and for reproducing various types of stable/meta stable phase diagrams, property diagrams, etc.

By means of optimization procedures, the coupling of the experimental thermodynamic information with phase diagram data can lead to optimal values of the thermodynamic properties of the various phases in the system. These procedures use all available experimental information on phase diagram and thermodynamic quantities like activities, enthalpies of formation and heat capacities. They are integrated in several software packages like BINGSS and TERGSS, PARROT, CHEMSAGE and FACT which are used worldwide provide an excellent representation of the thermodynamic properties of the properties of the various phases of a system and are consistent with phase diagram information.

The optimization of a system based on different types of data usually is done by trial and error methods. With increasing number of components and/or increasing number of

different types of data, this method becomes more and more cumbersome. Therefore a straight forward method is desirable. As straight forward method, the least squares method of Gauss was adapted [20].

In PARROT module of Thermo-Calc phase diagram is calculated for several times during the assessment to interpolate the thermodynamic properties between the experimental points and calculated data. During optimization which is by least-squares a set of experimental data is used.

This thesis describes the step by step procedure of calculating the phase diagram of AMPL-TRIS using CALPHAD models and Thermo-Calc computer program. The G-X curves were constructed for each phase derived from the Gibbs energy equations of pure components in unmixed condition. Gibbs energy minimization of the phases and the common tangent construction showing the two phase equilibrium is also discussed. Description of phase relations and thermodynamic data of the system has been obtained by means of thermodynamic modeling. A systematic description of Optimization method with PARROT module of Thermo-Calc is reported. Rigorous calculations and reanalysis of phase diagram have been done before presenting them.

1.6. References

[1] Mohammed M. Farid, Amar M. Khudhair, Energy Conversion and Management 45 (2004) 1597-1615.

[2] M.Telkes, Thermal storage for solar heating and cooling, Proceedings of the Workshop on Solar Energy Storage Subsystems for the Heating and Cooling of Buildings, Charlottesville (Virginia, USA), 1975.

[3] D. Chandra and W. Ding; U.S.Department of Energy Conference Proceeding CONF – 890351, 1989, 58-74.

[4] D. Chandra, H. Mandalia, and J. Hansen, Thermal Energy Storage in Phase Change Materials with On-Demand Heat Release, Final Report DOE Contract No. 19X-SL974V, Jan. 1994.

[5] A. Ter-Gazarian, Energy Storage For Power Systems, Peter Peregrinus L.T.D, p1-10, 57-73, 1994.

[6] D. Chandra, Crystal Structure Changes in the Solid-Solutions of Pentaglycerine-neopentlyglycol, Final Report to Solar Energy Research Institute, Midwest Research Institute, Golden Colorado, 1986.

[7] Timmermans. J., J. phys. Chem. Solids, 1961, 18(1), 1-8.

[8] B. zalba et al., Applied Thermal Engineering , 23 (2003) 251-283.

[9] D. Chandra, W.M. Chien, V. Gandikotta, D.W. Lindle, Z., Phys. Chem., 216 (2002) 1433-1444.

[10] Suresh Divi, Raja Chellappa, Dhanesh Chandra, J. Chem. Thermodynamics, 38 (2006) 1312-1326.

[11] Dhanesh Chandra, Raja Chellappa, Wen-Ming Chien, Journal of Physics and Chemistry of Solids, 66 (2005) 235-240.

[12] Raja Chellappa, Renee Russel, Dhanesh Chandra, Computer Coupling of Phase Diagrams and Thermochemistry, 28 (2004) 3-8.

[13] Raja Chellappa, Dhanesh Chandra, Computer Coupling of Phase Diagrams and Thermochemistry, 27 (2003) 133-140.

[14] M. Barrio, J.Font, D.O. Lopez, J. Chem. Phys., 91 (1994) 189-202.

[15] Zhang Zhi Ying , Yang Meng Lin, J. Chem. Thermodynamics, 22, (1990) 617-622.

[16] B. Meurer, P.J. Spencer, Thermocalc & Dictra, Computational tools for Materials Science, CALPHAD, 26 (2002) 139-143.

[17] B. Sundman, B. Jansson and J-O. Andersson, CALPHAD, 9 (1985) 153.

[18] B. Jansson, M. Sachalin, M.Selleby and B.Sundman in Computer Software in Chem. Extract. Metall., C.W. Bale and G.A. Irons, Editors, The Met Soc. Of CIM, Quebec (1993) 57.

[19] THERMO-CALC user manual.

[20] H.L Lukas, E.Th. Henig, and B. Zimmermann, CALPHAD, 1.1 (1977) 225-236.

[21] V. Kamisetty, Pressure-Temperature Phase Diagram Of Tris (Hydroxymethyl) Aminomethane And Phase Diagram Determination Of Tris(Hydroxymethyl)Aminomethane − 2-Amino-2-Methyl-1, 3-Propanediol(AMPL) Binary System, M.S Thesis, University of Nevada, Reno, 2010.

CHAPTER 2

CALPHAD modeling of Phase Diagrams

2.1. Introduction to Phase Diagram Calculation

Thermodynamics is the basis of materials science and engineering. It has been a major contribution to the design of new materials in metallurgy. Calculation of phase diagrams for multi-component systems using a thermodynamic approach is an important step in resolving industrial problems. The relationship between the composition, microstructure, and process conditions, phase diagrams are used in materials research. For the development of new materials there is always demand of new applications for achieving quality. The design of new materials to achieve the optimal desired properties is predominately achieved by the advances in computational materials science and information technology.

Different approaches of determining a phase diagram:

- Common Tangent Method
- Analytical Method
- Equation of State Method
- Equilibrium Constant Method
- Calphad Method

Where in which, the CALPHAD approach is currently the most widely used because of the ease with which equilibrium computations can be coded using a computer.

The CALPHAD approach is based on mathematically formulated models describing the thermodynamic properties of individual phases. The model parameters are evaluated from thermo chemical data of individual phase equilibrium data between phases. Generally in practical applications of materials during CALPHAD modeling, the commonly controlled processing variables are temperature (T), pressure(P), and number of atoms or moles of component i(Ni) which render the Gibbs energy (G) to be the state function to be modeled as T, P and Ni.

2.2. Gibbs energy Modeling of Solution Phase

A number of models are available for the thermodynamic properties of various phases. The integral Gibbs energy will be used as the modeled thermodynamic property. Since the experiments are generally carried out at constant temperature and pressure it is practical to model Gibbs energy than any other thermodynamic function. The traditional 'Monte Carlo' method for thermodynamic calculations is not being used in Calphad.

Each type of phase has different physical and chemical properties and structures which requires different types of models for them to describe accurately. Since those mathematical expressions are in more general form sometimes the mathematical expressions describing a physical quantity may be similar to the expressions of the other. These general expressions must have to be able to incorporate in them the additional phase properties or behavior involving chemical ordering, magnetic ordering and order-disorder transitions. One can independently select models for the phases except only when phases are of same structure family.

There are two types of Gibbs energies, configurational Gibbs energy due to mixing of unlike atoms and Gibbs energy due to bonding between the molecules.

The selection of the model for a phase must be based on the physical and chemical properties of the phases, for example crystallography, type of bonding, order-disorder transitions, and magnetic properties [3]. The phase equilibria and the thermodynamic properties measured for a system are incorporated in to the Gibbs energy model parameters adjusted so as to explain the system thermodynamically. The term parameter will be used for a quantity that is part of a model, like excess parameter. Some parameters can be a function of temperature, pressure, or even composition, and thus can be split into several other parameters. Each parameter may consist of several coefficients and a coefficient is always just a single numerical value.

The general form of a phase theta is expressed as

$$G_m^{\theta} = {}^{\text{srf}}G_m^{\theta}$$

In order to predict the multiphase equilibria or to analyze industrial process thermodynamic calculations are used initially. Modeling is a connection between experimental observations and theoretical predictions and is preceded with the minimization of the total Gibbs energy of a system (1). Many models empirical or derived from statistical thermodynamics have been published. There exist a number of models to evaluate the thermodynamic behavior of the solution phases, non-stoichiometric compounds with different structures, or phases with order-disorder

transformations [2]. In the Calphad modeling, the molar Gibbs energy of individual phases is modeled.

2.2.1. Substitutional Solution models

The thermodynamic description of Substitutional solutions in terms of power series have been formulated by many mathematicians like Margules [4], Redlich and Kister [5], Esdaile[6], Sharkey[7], Bale and Pelton [8] and Tomiska [9].

These power series have been extended to multicomponent system [6] following composition variable be used:

$$v_{ij} = (1 + (1 - m)x_i - \sum_{j \neq i}^{m} x_j)/m \qquad (2.1)$$

Where $\sum v_{ij} = 1$ whatever the order of the system, and a certain symmetry for the mole fractions is introduced.

Van Laar [10], Sactchard-hamer [11], Flory-Huggins [12, 13], Wolhl [14], and Wilson [15] suggested volume fractions as compositions instead of using molar fractions. The table [1] shows the thermodynamic properties of binary and ternary organic mixtures but very seldom for metallic solutions.

Equation	*Ref.*	*excess function*	*Comments*
Margules	(1)	$\sum_{i=0}^{\nu} a_i x^{\nu}$	
Redlich – Kister	(2)	$\sum_{i=0}^{\nu} a_\nu (x_i - x_j)^{\nu}$	$x_i + x_j = 1$
Esdaile	(3)	$x_A x_B [\sum_\nu (A1_{1(\nu+1)} x_A^{\nu-1} x_B + \sum_\nu (A2_{2(\nu+1)} x_A x_B^{\nu-1}]$	
Sharkey et al	(4)	$x_A x_B (\alpha_1 x_A + \alpha_2 x_B - \alpha_3 x_A x_B)$	
Legendre series	(5)	$\sum_{n=0}^{p} q_n P_n(x)$	P_n(*Legendre polynomials*) $P_0 = 1$ $P_1 = 2x - 1$ $P_n(x) = [(2n-1)(2x-1)/n] P_{n-1}(x) - [(n-1)/n] P_{n-2}(x)$
T.A.P. series	(6)	$(1 - x) \sum_{n=1}^{N} C_n x^n$	
Krupkowski	(9)	$\alpha(x - x^n)$	*equivalent to Hoch – Arpshofen equation* (10)
Van Laar	(11)	$\sum_{ij} a_{ij} z_i z_j$	$z_i = p_i x_i / \sum_j p_j x_j$ p_i : *constants* $S^{xs} = 0$
Scatchard – Hamer	(12)	$\sum_{ij} a_{ij} z_i z_j$	$z_i = V_i x_i / \sum_j V_j x_j$ $S^{xs} = 0$
Flory – Huggins	(13, 14)	$\sum_i^n x_i ln(\phi_i / x_i)$	ϕ_i : *volumefraction of* i
Wohl	(15)	$\sum_{ij} a_{ij} z_i z_j$	q_i : *effective molar volume of* i V_i : *molar volume of* i
Wilson	(16)	$-\sum_i^n x_i ln[\sum_{j=1}^n x_j \Lambda_{ij}]$	$H_m = 0$

Table 2.1. Analytical equations representing the Excess Gibbs Energies of Substitutional Solutions [16].

The solubility of the one or more components in a phase is said to be solution phase. There exist four major types of solution phases in CALPHAD software programs:

1. Random Substitutional
2. Sublattice
3. Ionic and
4. Aqueous

For all solution phases the Gibbs free energy is given by,

$$G = G^{o} + \Delta G_{mix}^{ideal} + G^{EX} \tag{2.2}$$

where G^{o} is the contribution of the pure components of the phase to the Gibbs energy, ΔG_{mix}^{ideal} is the ideal mixing contribution and G^{EX} is the contribution due to the non-ideal interactions between the components known as the Excess Gibbs Energy.

2.2.2. Gibbs Energy for Pure Species or Stoichiometric Compounds

The integral Gibbs energy, $G(T,P)$ of a pure compound or species is given by the following simple equation,

$$G(T,P) = H(T,P) - TS(T,P) \tag{2.3}$$

The enthalpies and entropies are represented as functions of temperature and pressure. In all the major databases such as Scientific Group Thermodata Europe (SGTE) Database, the Gibbs energy is usually of the form,

$$G_m(T) - H_m^{SER} = a + bT + cT\ln(T) + \sum_{2}^{n} d_n T^n \tag{2.4}$$

This is the Gibbs energy relative to the Standard Element Reference (SER) Enthalpy of the element or substance at 298.15 K. The coefficients, *a*, *b* and *c* are determined from experimental data. For compounds for which such data is not available, we can derive the relation for $G(T,P)$ if we have the specific heat capacity as a function of temperature by using common thermodynamic relationships,

$$G(T) = H^{o}_{298} + \int_{298}^{T} C_P(T)dT - T\left(S^{o}_{298} + \int_{298}^{T} \frac{C_P(T)}{T}dT \right) \tag{2.5}$$

When the standard enthalpy and entropy of formation of compounds is not available they can be estimated using Group Contribution Techniques (Organic Compounds) or *Ab-initio* and statistical mechanics considerations.

2.2.3. Random Substitutional Models

Random Substitutional models are used for phases such as the gas phase or simple metallic liquid and solid solutions where components can mix on any spatial position, which is available to the phase. This is especially true in case of gas and liquid phases where the crystallographic structure is lost and there is no preferential occupation of any site by any particular component.

Simple thermodynamic models that account for non-ideality and mixing effects are grouped under this category. The gas phase and condensed phase modeling is presented in detail here.

- ***Mixing in Liquid and Solid Phases***

To model the liquid and solid Phases, we develop the concept of activity. Activity is defined in terms of fugacity. We note here that this definition is for convenience so that we maintain the functional form. The activity of a component 'i' in a mixture is defined as,

$$a_i = \frac{\hat{f}_i}{f_i^o} \tag{2.6}$$

Where $\hat{f}_i$ is the fugacity of component 'i' in solution phase and f_i^o is the fugacity of the pure component at temperature T.

Ideal Raoultian Solution

If the vapor in equilibrium with the condensed solution is ideal then

$$\hat{f}_i = p_i \qquad \text{and} \qquad f_i^o = p_i^o \tag{2.7}$$

$$\overline{G}_i - G_i = RT \ln(a_i) \tag{2.8}$$

For a solution that obeys Raoult's Law,

$$\overline{G}_i - G_i = RT \ln\left(\frac{p_i}{p_i^o}\right) = RT \ln(X_i) \tag{2.9}$$

or

$$a_i = X_i \tag{2.10}$$

Non-ideal Henrian Solution

When the condensed phase does not behave ideally, we introduce an activity coefficient to account for the non-ideality. The activity coefficient is defined as,

$$\gamma_i = \frac{a_i}{X_i} \tag{2.11}$$

When the activity coefficient is assumed as a constant parameter at infinite dilution, the solution is then called Henrian.

$$a_i = \gamma_i^o X_i \tag{2.12}$$

The Gibbs energy of a binary solution mixture is given by,

$$G = X_A \overline{G}_A + X_B \overline{G}_B \tag{2.13}$$

The Gibbs energy of unmixed pure components is given by,

$$G^o = X_A G_A^o + X_B G_B^o \tag{2.14}$$

The change in Gibbs energy for binary can be written as,

$$G - G^o = \Delta G^{Mix} = RT\left(X_A \ln\left(a_A\right) + X_A \ln\left(a_B\right)\right) \tag{2.15}$$

For a solution with ‘n’ components the general equations can be written as,

$$G = \sum_i X_i \overline{G}_i \tag{2.16}$$

$$G^o = \sum_i X_i G_i^o \tag{2.17}$$

$$G - G^o = \Delta G^{Mix} = RT \sum_i X_i \ln(a_i) \tag{2.18}$$

We can divide the Gibbs energy of mixing into the ideal and excess parts, where the excess Gibbs energy will be the part that accounts for non-ideality.

$$\Delta G^{Mix} = \Delta G_{ideal}^{Mix} + G^{EX} \tag{2.19}$$

$$G = G^o + \Delta G^{Mix} = G^o + \Delta G_{ideal}^{Mix} + G^{EX} \tag{2.20}$$

Substituting eqns. (2.9), (2.10) and (2.11) into eqn. (2.18), we can obtain the expression for different models which are shown below,

Ideal Solution Model

$$G = G^o + \Delta G_{ideal}^{Mix} = G^o + RT \sum_i X_i \ln(X_i) \tag{2.21}$$

$$G^{EX} = 0 \tag{2.22}$$

Henrian Solution Model

$$G = G^o + \Delta G^{Mix} = G^o + RT \sum_i X_i \ln(X_i) + RT \sum_i X_i \ln(\gamma_i^o) \tag{2.23}$$

$$G^{EX} = RT \sum_i X_i \ln(\gamma_i^o) \tag{2.24}$$

General Non-ideal Solution Model

$$G = G^o + \Delta G^{Mix} = G^o + RT\sum_i X_i \ln(X_i) + RT\sum_i X_i \ln(\gamma_i) \quad (2.25)$$

$$G^{EX} = RT\sum_i X_i \ln(\gamma_i) \quad (2.26)$$

Eqns. (2.25) and (2.46) are the most general equations that model the non-ideal solution. The semi-empirical approaches of Activity Coefficient modeling is the preferred way of Chemical Engineering community.

2.2.4 Regular Solution Model

The regular solution model is the simplest of the non-ideal models and considers that the magnitude and sign of interactions between the components in a phase are independent of composition. The discussion presented here follows the classic undergraduate text for metallurgical thermodynamics by Gaskell [19]. Assuming the total energy of the solution E_0 arises from only the nearest-neighbors bond energies in a binary system A – B, we can express this as,

$$E_0 = \omega_{AA}E_{AA} + \omega_{BB}E_{BB} + \omega_{AB}E_{AB} \quad (2.27)$$

where $\omega_{AA}, \omega_{BB}, \omega_{AB}, E_{AA}, E_{BB}, E_{AB}$ are the number of bonds and energies associated with formation of different bonds types AA, BB and AB. If there are N atoms in solution and the co-ordination number for nearest neighbors of the crystal structure is *z*, the number of bond types being formed in a random solution is,

$$\omega_{AA} = \frac{1}{2} NzX_A^2 \tag{2.28}$$

$$\omega_{BB} = \frac{1}{2} NzX_B^2 \tag{2.29}$$

$$\omega_{AB} = NzX_A X_B \tag{2.30}$$

Where X_A and X_B are the mole fractions of A and B. Substituting eqns. (2.28), (2.29) and (2.30) into eqn. (2.27),

$$E_0 = \frac{Nz}{2}\left(X_A E_{AA} + X_B E_{BB} + X_A X_B \left(2E_{AB} - E_{AA} - E_{BB}\right)\right) \tag{2.31}$$

Assuming pure A and B as reference states, eqn. (2.31) can be rewritten as,

$$H_{Mix} = \frac{Nz}{2}\left(X_A X_B \left(2E_{AB} - E_{AA} - E_{BB}\right)\right) \tag{2.32}$$

Using this enthalpy of mixing, we can write the Excess Gibbs energy of mixing as,

$$G^{EX} = X_A X_B \Omega \tag{2.33}$$

Here Ω is a temperature dependent interaction parameter usually represented as,

$$\Omega = A + BT \tag{2.34}$$

Combining eqn. (2.33) with eqn. (2.20), we can write the final equation for the Gibbs Energy for a regular solution with ‘n’ components,

$$G = G^o + RT\sum_i X_i \ln\left(X_i\right) + \sum_i \sum_{j>i} X_i X_j L_{ij} \tag{2.35}$$

Now all that remains to be done is improve upon the assumption of composition independent interactions. Many improvements have been proposed and this leads to the different models, one particular model is shown in eqn. (2.39).

2.2.5. The Substitutional-Regular-Solution Model

Regular and sub-regular solution models are applied in calculation of the phase diagram for the random substitutional phases such as gas phase or metallic liquid and solid solutions where the mixing of atoms or their occupation can take place in any position in the lattice site.

The excess Gibbs energy for a sub-regular solution model is given by

$$\Delta H_{mix} = \Delta G_{mix}^{xs} = X_1 X_2 [\alpha_0 X_1 + \alpha_1 X_2] \quad (2.36)$$

The regular solution model is so flexible that we can add up the additional parameter with each term to the heat of mixing equation.

For the non-regular solution model the above equation can be formulated by adding the dependency of the enthalpy of the mixture on temperature as follows

$$\Delta H_{mix} = \Delta G_{mix}^{xs} = X_1 X_2 [\alpha_0(T) X_1 + \alpha_1(T) X_2] \quad (2.37)$$

Redlich-Kister Model

The multi-component solution widely applied for such models is the Redlich-Kister equation.

$$\Delta G_{mix}^{xs} = \sum_{i=1}^{c} \sum_{j>1}^{c} X_i X_j \sum_{v=0}^{n} L_{ij}^{v} \, (X_i - X_j)^v \quad (2.38)$$

Adding more complex composition dependency to L,

$$G = G^{o} + RT\sum_{i} X_i \ln(X_i) + \sum_{i}\sum_{j>i} X_i X_j \sum_{v} L_{ij}^{v}\left(X_i - X_j\right)^{v} \tag{2.39}$$

The first term on the right hand side of the equation (2.39) contributes to the Gibbs energy due to the mechanical mixing, and the second on the ideal mixing and the third indicates the deviation from ideal mixing also specified as excess Gibbs energy mixing. L_{ij}^{v} represent the interaction parameters between the atoms for a given occupancy of the other and they can be described by the Redlich-Kister type polynomial derived for each of the binary systems. They are interaction parameters either constants or linearly dependent on the temperature and exponent *v*. the model becomes regular when *v*=0 and sub-regular when *v*=1.

The models described in the Calphad consider the sublattices which are characterized by different crystallographic symmetries. A sublattice is a division of a crystal characterized by different crystallographic symmetries. Sublattice can either be a single constituent or a compound formed by each constituent from each sublattice. Such compound can be stoichiometric composition. The so called end members of a solution phase have such compounds. The phase having single set of sites and the elements as constituents is said to be pure element [3]. The end members consisting of such compounds have solubility limit.

2.3. Experimental Data for Optimization

Calculated results when combined with the experimental data using the modeling methods like Calphad one can find the loop holes in the trends of the theoretical applications

As we know that the experiments are quite expensive when compared to the theoretical applications the collected data from the literature survey should be validated by optimizing the data to get the preliminary phase diagram before beginning with one's own experimental data. This always helps in investigating the phases with inadequate data leading to more experimentation.

More information related to the phase-diagram and thermodynamic functions can be obtained from the literature review. It is still of great importance to know the experimental methods used for measuring the heat capacity data, enthalpy and transition temperatures. The experimental data can be divided in to thermodynamic data, and phase-diagram data.

Binary Phase-Diagram Data

The experimental data points can be found to measure the binary phase diagram are

i) The temperatures at invariant three phase equilibria points

ii) The points on the two- phase field boundaries

iii) For the samples of single and two phase regions with composition x annealed to equilibrium at constant temperature T.

iv) the values calculate through the least-squares method which include the calculated temperature for which the amounts of three phase and pressure are given, the temperature of two-phase equilibrium for which the composition of once phase, the amounts of two phases and the pressure are given, the composition of one phase in the two-phase equilibrium at given temperature and pressure.

Thermodynamic Data

The *calorimetric data* gives the physical and chemical changes heat capacity of a system. The change in temperature before and after a chemical reaction between the reactants added to the calorimeter is measured and then multiplied with the specific heat and mass of the reactants gives the energy given off or absorbed during that reaction.

Chemical –potential data are connected with a formula $\Delta\mu = RTln(a)$ in which Δμ is the difference of chemical potentials at two different equilibrium states

2.4. Phase Diagram Determination

Given a system in which the components can co-exist in many phases, we are usually interested in the Temperature – Composition relationships (*T* versus *x*). There are many different methods to evaluate equilibrium conditions in multicomponent systems and the Gibbs free energy curves forms the basis for doing these calculations. The prevalent approaches are:

Gibbs energy minimization methods for calculation of phase equilibria can be conducted in following prevalent methods:

- Graphical and Numerical Common Tangent Construction Approach
- Analytical Approach
- Equation of State (EOS) Approach
- Equilibrium Constant Approach (ECA)
- CALPHAD Approach

Of these approaches, the CALPHAD approach is currently the most widely used. This is primarily dictated by the ease with which it can be coded to perform the calculations using a computer. A summary of 3 of these different approaches will be provided here to compare and contrast with the CALPHAD approach.

2.4.1. Construction of common tangent for a binary system

This is the most intuitive of all the methods. It is an earlier method of calculating a phase diagram. In a binary system to derive equilibrium phase boundary compositions over a range of temperatures, and produce a complete phase diagram, the calculation of common tangents to the Gibbs energy curves of the phases can be conducted. For ternary system the calculation of the points of contact of tangents to the Gibbs energy curves becomes difficult and time consuming. Gaye and Lupis described the Gibbs energy minimization methods for calculation of phase equilibria in higher order systems. An example using a hypothetical binary system (A – B) will be shown here. This particular system assumes that the solid and liquid phases follow Regular Solution behavior.

1. The conditions for the two phase field equilibrium in a binary system:

$T^{\alpha} = T^{\beta}$ $P^{\alpha} = P^{\beta}$ $\mu_1^{\alpha} = \mu_1^{\beta}$ $\mu_2^{\alpha} = \mu_2^{\beta}$

If two phases are in equilibrium, the Partial Molar Gibbs free energy of a component is equal is both the phases. For example, in a two-phase region of solid – liquid equilibrium, this condition can be represented as:

$$\overline{G}_A^{Liq} = \overline{G}_A^{Sol} \tag{2.40}$$

Where,

$$\overline{G}_A^{Liq} = \left(\frac{\partial G^{Liq}}{\partial x_A}\right)_{T,P} \text{ And } \overline{G}_A^{Sol} = \left(\frac{\partial G^{Sol}}{\partial x_A}\right)_{T,P} \tag{2.41}$$

2. For a given T and P, the stable phase is the one which has the minimum Gibbs free energy.

A graphical representation of the common tangent construction is illustrated in Fig. 2.1 the diagram is constructed at constant temperature and pressure. The G-X curves represent the thermodynamic behavior of the solutions. As the G-X curves for the two phases cross with each other, it is possible to construct a common tangent line to both curves. The points of contact of the tangent and the curves are X_2^{α} and X_2^{L}, a unique pair of composition.

Applying the same principle to a system exhibiting the regions of stability for two different phases, Fig 2.2. The compositions at N and P exists in two phase equilibrium. X_2^0 lying between X_2^{α} and X_2^{L}. The point M represents the free energy of mixing for the composition X_2^0

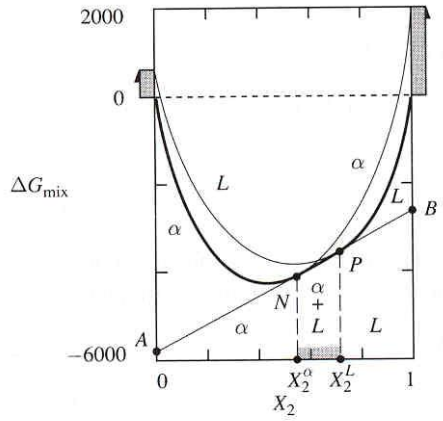

Fig 2.1. The G-X curves for two different phases are plotted with consistent reference states. If these curves cross, then unique line can be drawn that is tangent to both curves. The comparisons at these tangent points satisfy the conditions for equilibrium between the phases [18].

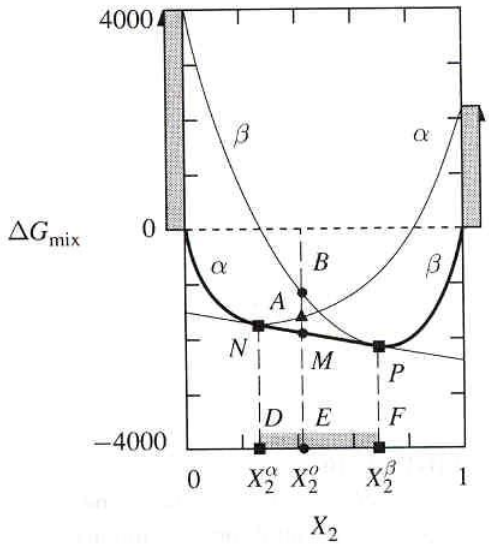

Fig 2.2 Consistent G-X curves are plotted for two phases, α and β. For any composition X_2^α and X_2^β has a lower free energy than either homogeneous phase at X_2^0, or any mixture of solution compositions other than X_2^α and X_2^β [18].

$\overline{AB}$ is the tangent line. The points A and B represents the Gibbs free energy of component 1 in α solution of composition X_2^{α} and at the same time gives the Gibbs energy of component 1 in a liquid solution composition X_2^{L}. These compositions at the two at opposite ends of the tie line phases represent the states of the two phases.

Generally a system can exhibit an arbitrary number of phases. Fig. 2.3. The combination of single and two phase regions given by the curve segments and common tangent lines trace the excess Gibbs free energy minimum. The line segment OA-AB-BC-CD-DE-EF-FP shows the trace.

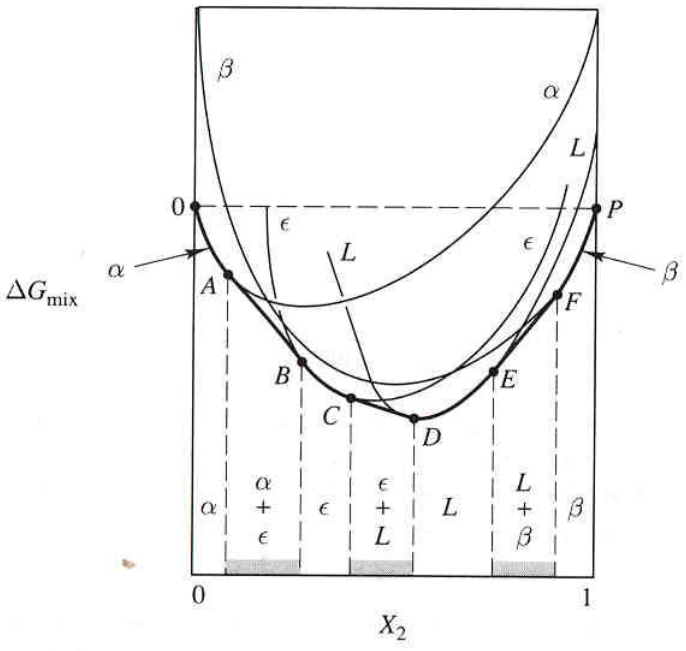

Fig 2.3. Taut string construction shows the sequence of equilibrium conditions across the composition range in a system forms, α, ε, *L* and β [18].

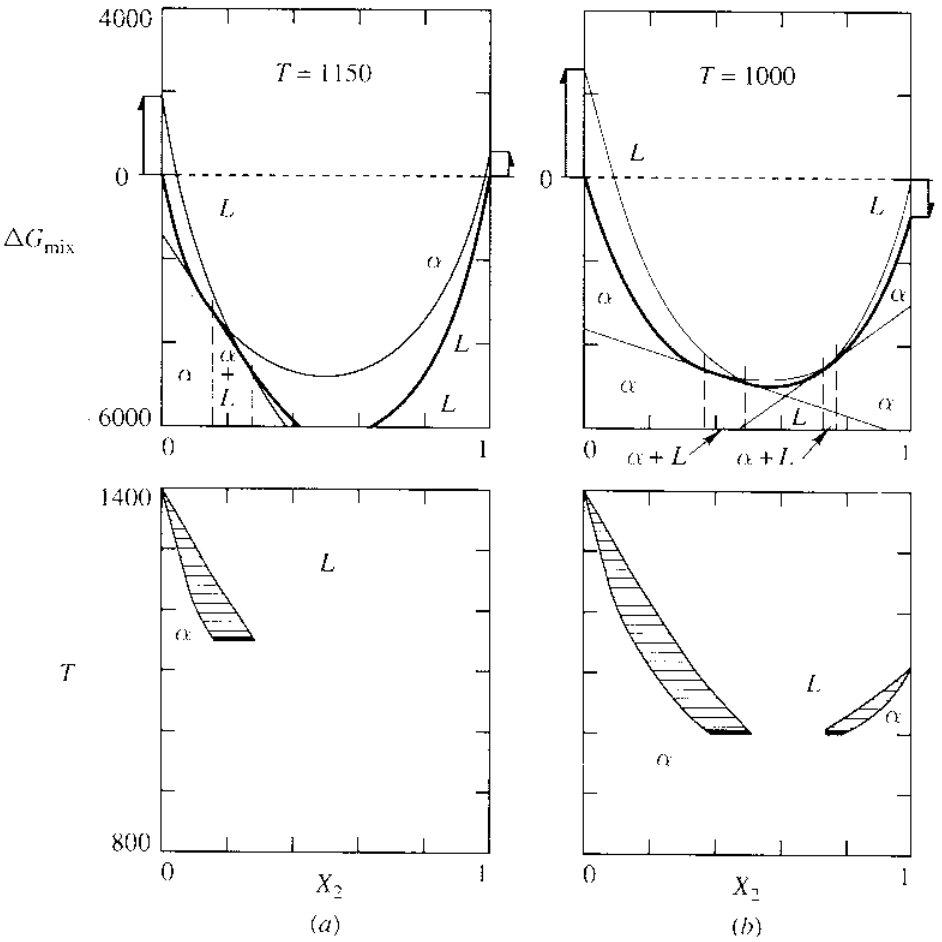

Fig 2.4a,b. Pattern of thermodynamic behavior that generates a two phase field with a minimum. $a_0^{\alpha} = 6000\ \left(\frac{J}{mol}\right);\ a_0^{\alpha} = -2000(j/mol)$[18].

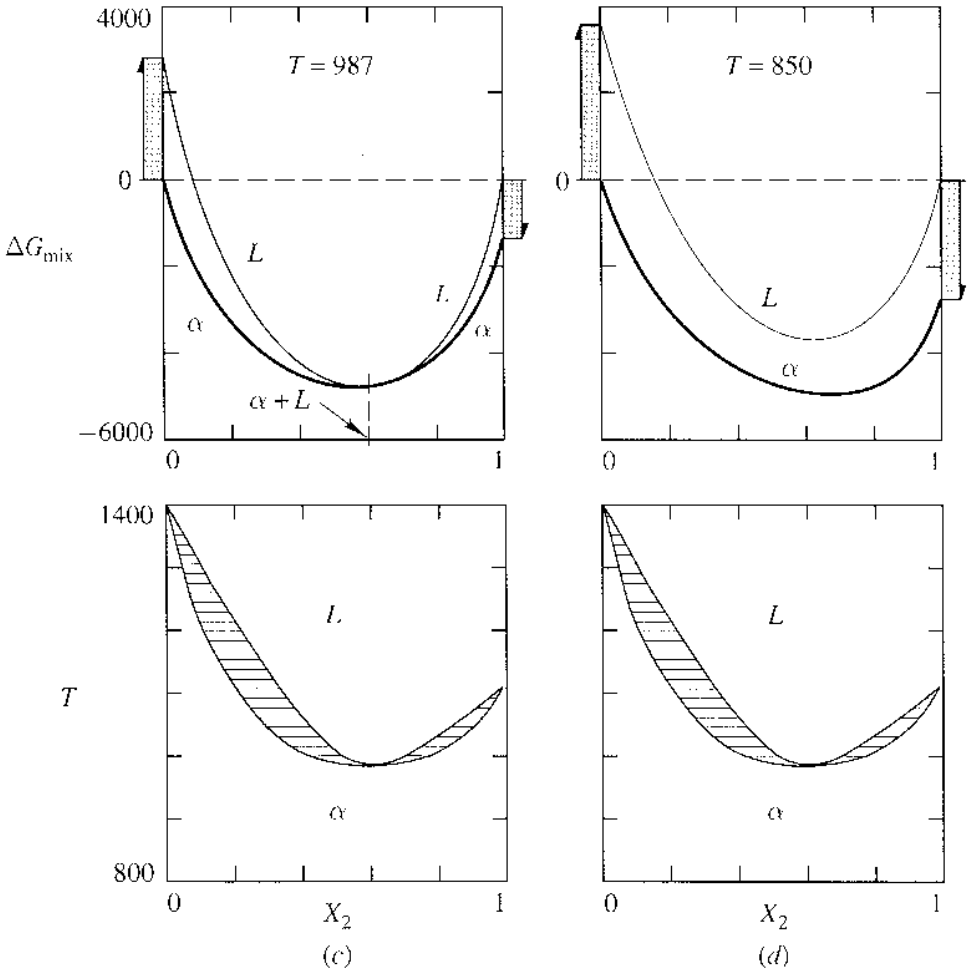

Fig 2.4c,d. Pattern of thermodynamic behavior that generates a two phase field with a minimum. $a_0^{\alpha} = 6000\ \left(\frac{J}{mol}\right);\ a_0^{\alpha} = -2000(j/mol)$[18].

The Fig 2.4. Shows a two phase field with a minimum together with a set of respective (G-X) diagrams. To generate the complete two phase field at a constant pressure binary diagram, repetition of the construction at a set of temperatures which is the span in which the diagram is plotted. During this construction two different come in to picture which can determine the configuration:

1. The mixing behavior of two phases which include excess and ideal energy mixing
2. The Gibbs energy variation between the stabilities of the two phases for the pure substances.

In simple binary system considered here the solid phase has a lower Gibbs free energy at T =900 K (*Fig. 2.4d*), so it is more stable than the liquid phase. At T = 987K (*Fig. 2.4c*) the liquid phase has equal Gibbs free energy as the solid, which can be projected as a line segment on the T-X diagram below it. At T = 1000 K (*Fig. 2.4d*), we can see that the liquid phase is stable for some mole fractions and the solid phase is stable for some mole fractions. It is obvious then that there are two a regions where the two phases can exist in equilibrium. At T = 1150 K (*Fig. 2.4a*) we can observe the two phase field. At higher temperatures only liquid phase exists.

The chemical equilibria constraints, eqns. (2.37) and (2.38) are written again below:

$$\overline{G}_A^{Liq} = \overline{G}_A^{Sol} \tag{2.42}$$

Where,

$$\overline{G}_A^{Liq} = \left(\frac{\partial G^{Liq}}{\partial x_A} \right)_{T,P} \text{ and } \overline{G}_A^{Sol} = \left(\frac{\partial G^{Sol}}{\partial x_A} \right)_{T,P} \tag{2.43}$$

$$x_A^{Liq} + x_A^{Sol} = 1 \tag{2.44}$$

Substituting eqn. (2.43) into (2.42),

$$f_1\left(x_A^{Liq}, x_A^{Sol}\right) = \overline{G}_A^{Liq} - \overline{G}_A^{Sol} = \left(\frac{\partial G^{Liq}}{\partial x_A}\right)_{T,P}\Bigg|_{x_A^{Liq}} - \left(\frac{\partial G^{Sol}}{\partial x_A}\right)_{T,P}\Bigg|_{x_A^{Sol}} = 0 \qquad (2.45)$$

Eqn. (2.55) is basically stating the fact that slopes of the curves at equilibrium composition are the same. There are two unknowns in eqn. (2.55), so we need another equation. By constructing lines defined by equilibrium compositions for both solid and liquid phases, we can see that the intercepts have to be equal (since it is the same line). The basic equation of the line is,

$$y = mx + b \qquad (2.46)$$

We can write this for both solid and liquid phases,

$$\overline{G}_A^{Liq} = \left(\frac{\partial G^{Liq}}{\partial x_A}\right)_{T,P}\Bigg|_{x_A^{Liq}} \bullet x_A^{Liq} + b \quad \text{and} \quad \overline{G}_A^{Sol} = \left(\frac{\partial G^{Sol}}{\partial x_A}\right)_{T,P}\Bigg|_{x_A^{Sol}} \bullet x_A^{Sol} + b \qquad (2.47)$$

From eqn. (2.61), we can equate the intercepts and get our second equation,

$$f_2\left(x_A^{Liq}, x_A^{Sol}\right) = \overline{G}_A^{Liq} - \left(\frac{\partial G^{Liq}}{\partial x_A}\right)_{T,P}\Bigg|_{x_A^{Liq}} \bullet x_A^{Liq} - \overline{G}_A^{Sol} - \left(\frac{\partial G^{Sol}}{\partial x_A}\right)_{T,P}\Bigg|_{x_A^{Sol}} \bullet x_A^{Sol} = 0 \qquad (2.48)$$

In eqns. (2.46) and (2.48), we have two sets of equations with two unknowns which can be solved graphically by drawing tangents (*Fig. 2.4*). This graphical method of finding the compositions is called the "common tangent" method. A magnified view is shown in *Fig. 2.5*. To solve graphically by drawing common tangents is cumbersome. We usually use numerical packages to solve these non-linear algebraic equations. We can approximate the differentials by using a forward or centered difference method.

Numerical packages like MathCAD, MATLAB have robust codes for solving algebraic equations.

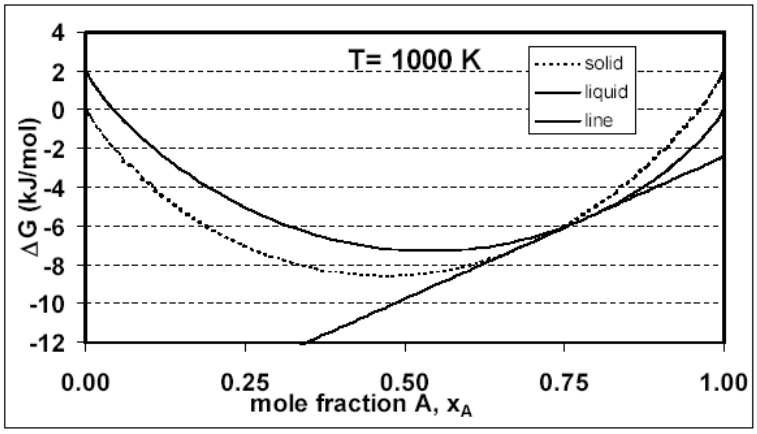

Fig 2.5a. Common tangent drawn to find equilibrium composition points for solid and liquid phases (Tie – line points)

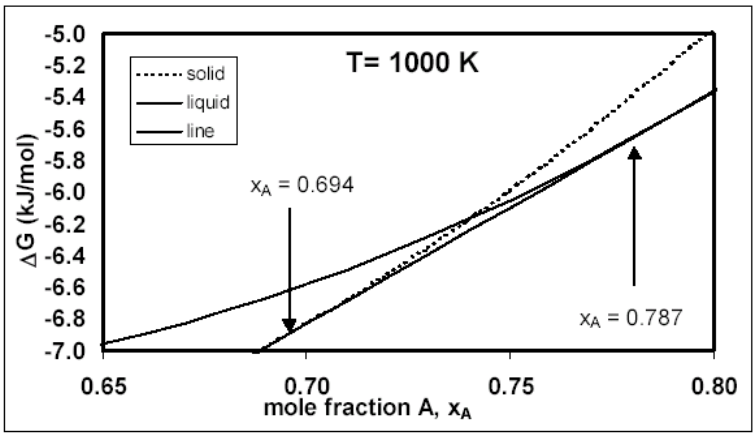

Fig 2.5b. Magnified view of *Fig.2.4*.

2.4.2. CALPHAD Approach

CALPHAD methods provide a true equilibrium calculation by considering the Gibbs energy of all the phases and minimizing the total Gibbs energy of the system (G). At the heart of the CALPHAD-method is the Gibbs energy modeling [3]. This involves selection of appropriate thermodynamic models for the Gibbs energy functions $G(P, T, x)$ of phases and maximum-likelihood estimation of the model parameters using critically selected thermo-chemical and constitutional data as input, eventually leading to an optimized thermodynamic description of the system. A flowchart representing the procedure of CALPHAD method is shown in *Fig. 2.6*.

The total energy G of the system is represented either in terms of the chemical potential of the component 'i', $\overline{G_i}$,

$$G = \sum_i n_i \overline{G_i} \tag{2.49}$$

or by the amount of phases (N^{Φ}) involved,

$$G = \sum_{\phi} N^{\phi} G^{\phi}{}_m \tag{2.50}$$

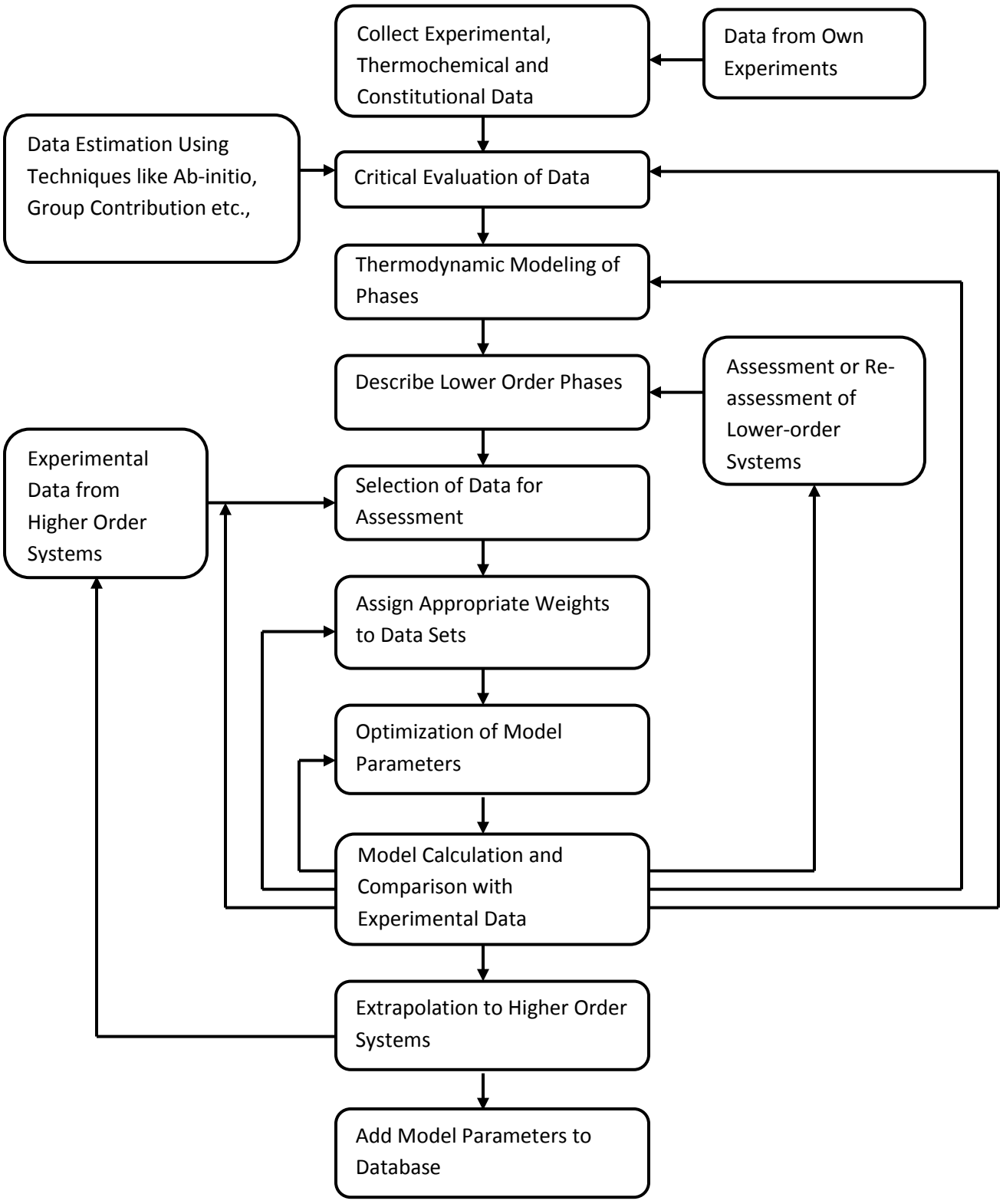

Fig 2.6. Schematic representation of CALPHAD method for Assessing Phase Diagrams [22].

This total Gibbs free energy is now minimized considering the phases present in multi-phase equilibria by using various numerical techniques. The main questions that arises in using this approach are,

1. What is the model (semi-empirical, theoretical or empirical) for Gibbs free energy that adequately represents the non-ideality of the phase under consideration? How many parameters do we need to include for the excess Gibbs energy to be modeled?
2. What is the minimization technique that is robust and provides good convergence for the model parameters?

The solution to these questions forms the basis for assessments of phase diagrams using the CALPHAD method. To answer the first question, we have to understand the nature of non-ideality in the solution phase. Various models have been proposed and used for different systems. For Metal – Hydrogen systems, the Virial EOS (for a given range of pressure) is usually proposed for Hydrogen in gaseous phase and the sublattice model for an approximate description of the solid hydride phase. The sublattice modeling is a very important feature and has been discussed in detail in *Section 3.3*.

2.5. Application of the CALPHAD

2.5.1. Description of the CALPHAD Procedure

CALPHAD (CALculation of PHAse Diagrams) as it thrives today is a technique to determine phase diagrams of alloys and multi-component systems that was pioneered in the 1960's and 1970's by Larry Kaufman among others [3]. This study provides an

introduction to the theory and applications of this methodology along with the computational software that are available. A brief summary of the underlying thermodynamics of phase equilibria calculations is given with some illustrations and many of the recent advances especially in the modeling of the solution phases will be elucidated. The working of two of the widely used software F*A*C*T (Facility for Analysis of Thermodynamics) and Thermo-Calc is also presented.

A simple binary Ni – Cu system is considered here. The phase diagram for this system is shown in *Fig. 2.7*. For ease of understanding the procedure is described in steps. The main aim is to find the minimum Gibbs energy for a mixture of f.c.c and liquid phases for an equilibrium composition x^e_{fcc} and x^e_{Liq} at a given temperature T. Obviously it is assumed that the model for the two phases are known. The procedure to determine how to obtain the model is described in the next section. These steps have been mathematically formulated specifically.

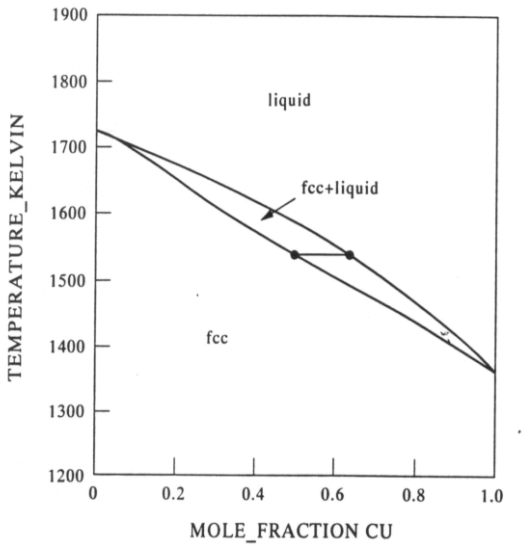

Fig 2.7. Ni-Cu Phase Diagram.

Step 1

Set Temperature as a constant (T = 1523K in this case)

Step 2

Define the total Molar Gibbs energy of the mixture using eqn. (2.49) as,

$$G_{Total} = \sum_{\phi} N^{\phi} G^{\phi}{}_{m} \tag{2.51}$$

with $N_i = \sum_{\phi} N_i^{\phi}$ and $\sum_{\phi} N^{\phi} = M$, where N_i is total number of moles of component 'i' in the system and N_i^{ϕ} is the number of moles of component 'i' in the phase ϕ and M is the total number of moles in the system. The above general equation is now written for our system as,

$$G_{Total} = N^{fcc} G_{fcc} + N^{Liq} G_{Liq} \tag{2.52}$$

$$N_{Ni} = N_{Ni}^{fcc} + N_{Ni}^{Liq} \tag{2.53}$$

$$N_{Cu} = N_{Cu}^{fcc} + N_{Cu}^{Liq} \tag{2.54}$$

$$N^{fcc} + N^{Liq} = M \tag{2.55}$$

Let us assume that the total number of moles is M = 1.

$$G_{Total} = G = X^{fcc} G_{fcc} + X^{Liq} G_{Liq} = N^{fcc} G_{fcc} + N^{Liq} G_{Liq} \tag{2.56}$$

Step 3

Find the composition at which the Gibbs energy for both the phases are equal. This is simply obtained from equating the molar Gibbs energy of the two phases.

$$G_{fcc} = G_{Liq} \tag{2.57}$$

Assuming that Liquid follows ideal solution behavior and the f.c.c phase follows regular solution behavior, eqn. (2.51) can be expanded as follows,

$$G_{fcc}^{o} = X_{Ni}^{fcc} G_{Ni}^{o,fcc} + X_{Cu}^{fcc} G_{Cu}^{o,fcc} = X_{Ni}^{fcc} G_{Ni}^{o,fcc} + \left(1 - X_{Ni}^{fcc}\right) G_{Cu}^{o,fcc} \tag{2.58}$$

$$G_{Liq}^{o} = X_{Ni}^{Liq} G_{Ni}^{o,Liq} + X_{Cu}^{Liq} G_{Cu}^{o,Liq} = X_{Ni}^{Liq} G_{Ni}^{o,Liq} + \left(1 - X_{Ni}^{Liq}\right) G_{Cu}^{o,Liq} \tag{2.59}$$

$$G_{Liq}^{EX} = 0 \tag{2.60}$$

$$G_{fcc}^{EX} = (A + BT) X_{Ni}^{fcc} \left(1 - X_{Ni}^{fcc}\right) \tag{2.61}$$

Substituting eqns. (2.58) – (2.61) into (2.57), we get

$$X_{Ni}^{fcc} G_{Ni}^{o,fcc} + \left(1 - X_{Ni}^{fcc}\right) G_{Cu}^{o,fcc} + RT\left(X_{Ni}^{fcc} \ln\left(X_{Ni}^{fcc}\right) + \left(1 - X_{Ni}^{fcc}\right) \ln\left(1 - X_{Ni}^{fcc}\right)\right) + (A + BT) X_{Ni}^{fcc} \left(1 - X_{Ni}^{fcc}\right) = X_{Ni}^{Liq} G_{Ni}^{o,Liq} + \left(1 - X_{Ni}^{Liq}\right) G_{Cu}^{o,Liq} + RT\left(X_{Ni}^{Liq} \ln\left(X_{Ni}^{Liq}\right) + \left(1 - X_{Ni}^{Liq}\right) \ln\left(1 - X_{Ni}^{Liq}\right)\right) + 0 \tag{2.62}$$

In eqn. (2.62), assuming,

$$X_{Ni}^{Liq} = X_{Ni}^{fcc} = X_0 \tag{2.63}$$

we have one equation in one unknown and we can solve this using any standard numerical package. From this X_0, shown in *Fig. 2.8*, we can calculate the amount of N^{fcc}. Using this as starting point has advantages of fast convergence though any point X_{Ni}, which would be the overall composition of *Ni*, satisfying the lever rule could be used.

$$N^{fcc} = \frac{\left| X_{Ni} - X_{Ni}^{Liq} \right|}{\left| X_{Ni}^{Liq} - X_{Ni}^{fcc} \right|} \tag{2.64}$$

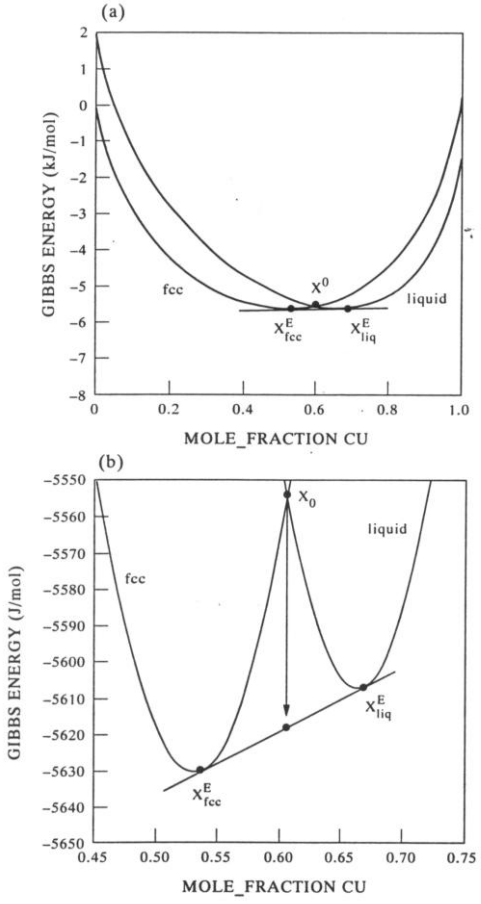

Fig 2.8. G/x curves for Ni-Cu system at T =1523 K.

Step 4

Assume alloy to be of single f.c.c phase and introduce an arbitrary amount of liquid. This can be done by,

$$N^{Liq} = N^{Liq} + \Delta N^{Liq} \tag{2.65}$$

If $N^{Liq} = 0$ to begin the minimization it is single phase (f.c.c), then addition of a small amount of liquid is carried out by adding ΔN^{Liq}.

Step 5

Retain mass balance by calculating new N^{fcc} based upon equations (2.54) – (2.55).

Step 6

Calculate the value of molar Gibbs energy using eqn. (2.56)

Step 7

Now, we keep N^{fcc} as a constant and start to vary N^{Liq} so that the value of Gibbs energy is reduced. This is a simple numerical iterative procedure that can be programmed easily. *Fig. 2.9* shows this iterative process starting from X_0.

Step 8

From *Fig. 12*, it is clear what we are accomplishing, the variation of *G* with respect to the amount of Liquid Phase, N^{Liq}. The iteration will stop when the value of the slope of the curve becomes zero. Numerically,

$$\frac{\partial G}{\partial N^{Liq}} <<< \xi \tag{2.66}$$

Where $\xi = 0.0001$ or some small number like that. This tolerance level or convergence limit, depends on the accuracy of computation we are trying to maintain. The differential (slope) can be approximated using a centered or forward difference approximation.

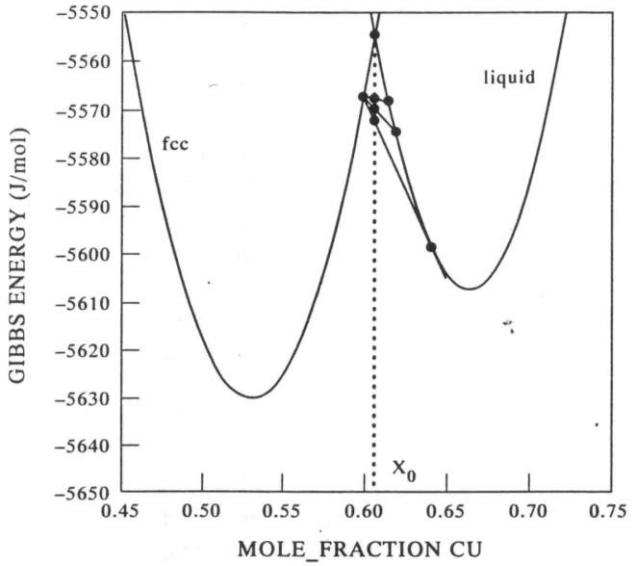

Fig 2.9. Iterative procedure starting from X_0 to find the minimum Gibbs energy by varying the amount of liquid phase, N^{Liq}, for the Ni –Cu binary system at T = 1523 K.

Step 9

The variation of N^{Liq} can be carried out in an arbitrary way but a better way of guessing the next amount of N^{Liq} to be added can be calculated more efficiently by calculating the second differential $\frac{\partial^2 G}{\partial N^{Liq\,2}}$. Plotting $\frac{\partial G}{\partial N^{Liq}} vs\, N^{Liq}$ gives us a clear picture of where the minimization of Gibbs energy is proceeding *(Fig. 2.11)*. Let the final value of *G* be $G(\text{fcc fixed, liquid variable})$

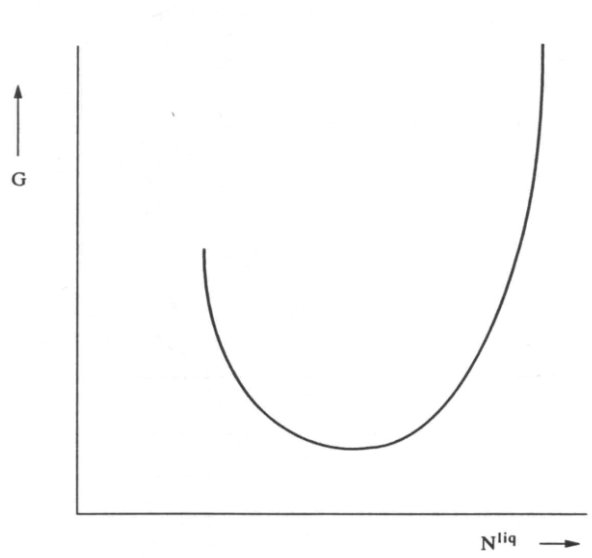

Fig 2.10. Determination of the end of the minimization routine.

Step 10

The composition of Liquid is held as a constant and the *Steps 4 – 9* are repeated for changes in f.c.c amount *(Fig 2.11)*. A new value of the final amount of minimized G is calculated. This is termed as $G(\text{liquid fixed, f.c.c variable})$.

Step 11

If,

$$G(\text{liquid fixed, f.c.c variable}) - G(\text{f.c.c fixed, liquid variable}) <<< \varepsilon \qquad (2.67)$$

where ε is some pre-determined convergence limit then we STOP the minimization process. If this is not achieved then Steps 4 – 11 are repeated. A schematic representation of the repetition is shown in *Fig. 2.13* and *Fig. 2.14*.

We will note here that the value of initial composition that was chosen was in the two-phase field, X_0 calculated from eqn. (2.64).

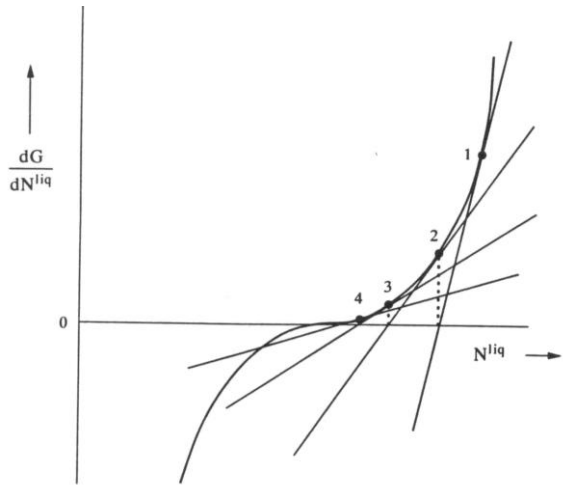

Fig 2.11. Schematic diagram of the first differential of the $G vs N^{Liq}$ curve

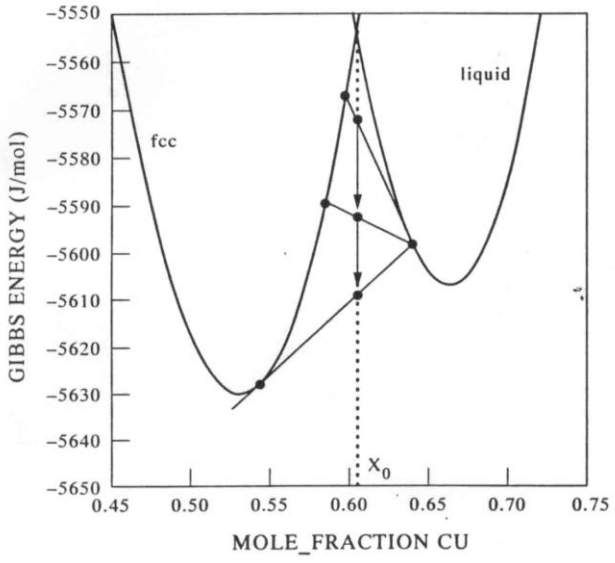

Fig 2.12. Schematic of the second iteration showing the variation of the f.c.c amount keeping amount of liquid fixed.

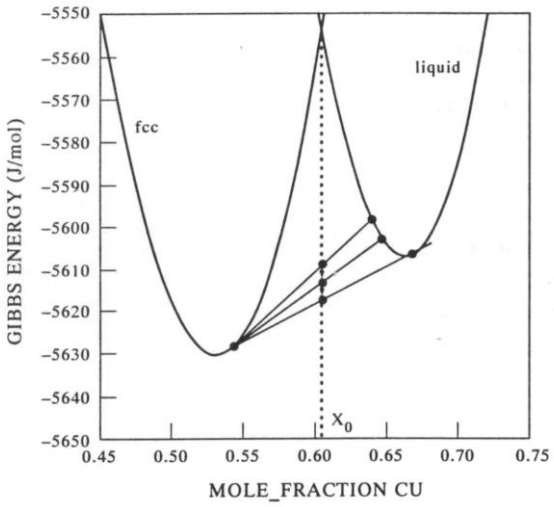

Fig 2.13. Repetition of Step 9, varying Liquid amount keeping f.c.c fixed, if Step 11 is not satisfied.

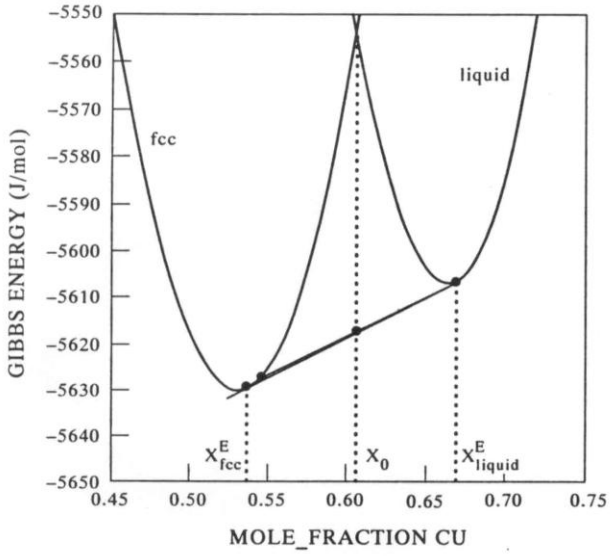

Fig 2.14. Repetition of Step 10, varying f.c.c amount keeping Liquid fixed, if Step 11 is not satisfied.

Step 12

If we start the iteration process using eqn. (2.65) that is from a single-phase field, the iterative schematic will look like *Fig. 2.15*. This will be automatically recognized by program. *Fig. 2.15 (a)* shows the case where the composition N^{fcc} was determined from eqn. (2.62) by assuming $X_{Ni} = 1 - X_1$. Now some amount of liquid is introduced and G is calculated.

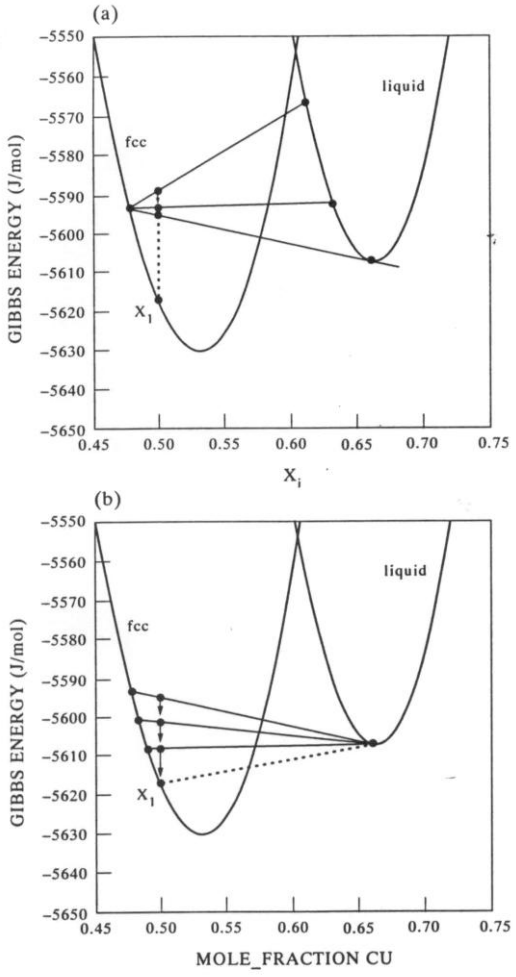

Fig 2.15. Minimization process starting from a single-phase field (f.c.c or Liquid)

The amount of liquid is then changed until a minimum value of G is obtained based upon eqn. (2.64) and this is noted to be $G(\text{fcc fixed, liquid variable})$. *Fig. 2.15 (b)* shows the case when N^{Liq} was determined from eqn. (2.65) and the minimization was done. The procedure is repeated (composition of f.c.c phase reaching X_1 and the amount of liquid is therefore reduced to zero to maintain mass balance. and the minimum value of G obtained is noted as $G(\text{liquid fixed, f.c.c variable})$. Step 11 is repeated to test for convergence. So, at the end of iteration from Step 4 – 11 what we have is just one single point on the phase diagram or a tie-line in the two-phase field. This procedure has to be repeated for various temperatures by changing the value of Temperature.

This will not be a computationally intensive procedure since there are only few numerical calculations involved. Three phase equilibria can also be calculated using a similar procedure. The procedure described above is a very general procedure for performing the Gibbs minimization. We can see that this is fundamentally different from ECA or EOS or the common tangent technique.

2.5.2. Minimization of Gibbs Free Energy Routines

The software program such as F*A*C*T (EQUILIB Module) and Thermo-Calc (POLY-3 Module) have customized routines to perform a similar minimization as described in the previous section. The concept is the same but the numerical techniques are advanced and robust.

The F*A*C*T program uses the method of steepest descent to provide a rapid solution to the minimization problem. The name of the code used is ChemSage. A Gibbs energy function is first defined by the following method.

$$G(Y) = \sum_i n_i G_i$$

$$\overline{G}_i\left(y_1^g, y_2^g ..., y_m^g, y_1^c, y_2^c, ..., y_s^c\right) = G_i^o + RT\ln\left(a_i\right) \qquad (2.68)$$

Y is the vector containing all the various compositions, m is the number of substances in gas phase and s is the number of substances in the condensed phase. A quadratic approximation of *G(Y)* is then expanded using the Taylor's approximation and minimized using the method of Lagrange multipliers. What we described in the previous section is basically a Newton – Raphson kind of method but new software program use more advanced numerical techniques. The Thermo-Calc software uses a similar technique in its POLY-3 module but these are proprietary in nature so I will not be able to discuss the particular routines in detail.

The methods like Newton-Raphson and steepest descent are based on calculating local minima. There are problems, which can arise when we are interested in determining minimum Gibbs energy for multi-component systems. There are techniques available, which can determine global to provide more robust estimates for the compositions at which the minimum Gibbs energy is obtained.

2.5.3. Model Parameters Determination through Thermodynamic Optimization

By means of optimization procedures, the coupling of the experimental thermodynamic information with phase diagram data can lead to optimal values of the thermodynamic properties of the various phases in the system. Thermodynamic optimization is the fitting process where the adjustable coefficients in the total Gibbs energy equation (These will essentially be the excess parameters such as $\Omega = A + BT$, A and B are the unknowns) are altered such that the best representation of both the experimentally measured phase diagram and thermodynamic properties are obtained. The accuracy with which these parameters are determined depends upon the mathematical form of the least squares technique. An optimization module is a part of any CALPHAD software, which takes various types of input such as

- Experimental Tie line Points
- Invariant Equilibria Points
- Enthalpy of Solution Phases
- Activity Measurements and Activity Coefficient Estimations
- Any Experimental Data that can be converted into "convenient" form

Currently F*A*C*T program does not have a robust optimization module. Thermo-Calc has the most robust code in its PARROT module. The general procedure for optimization at the present time using modules such as PARROT is performed through a process of trial-and-error by reducing the error using some mathematical algorithm. The manual

procedure is just that we change the excess parameters according to our personal judgment depending upon our knowledge of the system we want to optimize.

2.6. Thermodynamic Optimization of Phase Diagrams

The optimization was carried by using a computer program THERMO-CALC [3]. The measured enthalpies of compounds and the phase diagram data are used as input to the program. The adjusting process of the coefficients in the Gibbs energy equations to best fit both experimentally measured phase diagram and thermodynamic properties. The accuracy of this representation can be defined mathematically through some form of least-squares algorithm, and this forms the basis for optimization software such as PARROT [20].

The primary governing principles in PARROT involves establishing a criterion for the best fit (usually by specifying an objective function), separating the data into sets of different accuracies and making a distinction between independent and dependent variables. The criterion for best fit is based on the well-known Maximum Likelihood Estimation (MLE) technique where the best estimates of the model parameters should maximize the likelihood function, L, for the N experimental observations,

$$L = \prod_{i=1}^{N} F_i\left(\bar{z}_i^{o}, \bar{w}_i\right) \tag{2.69}$$

where F_i is the multivariable density function for the distribution of the measured values in experiment 'i', $\bar{z}_i^{o}$, are the measured experimental values which might differ from their

true value and $\bar{w}_i$ is used to denote the statistical parameters in the probability density function concerning experiment 'i' (Say measurement of Enthalpy of solution phase). The mathematical details of MLE type estimation are complex but a thorough understanding is vital to know the working of the PARROT module. It is suffice to say that the PARROT can accept any kind of experimental information in the evaluation of model parameters.

A strong statistical knowledge is necessary to understand the difference between the presence of systematic and random errors. The assumption of Gaussian distribution in the experimental data is reasonable though depending upon the uncertainty in the measurements other distributions may also be considered. But it is a well-known fact in the CALPHAD community that the Thermo-Calc software is very robust software and understanding the working should enable us to optimize the model parameters in a satisfactory manner.

2.6.1. Least-Squares Method of Optimization

This section is first introduced by gauss and can be found in many text books. This method is well known for optimization of single functions and also for the determination of the partial free enthalpy from binary phase diagrams. With the least squares method the simultaneous calculation of the different thermodynamic functions an be achieved. An analytical formalism is necessary which describes the different functions with coefficients taken from one common set of coefficients. Thermodynamic consistency is still well expressed by the use of thermodynamic relations. Following is the description

of our problem in terms of least-squares equations. In Gaussian calculation one equation of error belongs to each experimental value. The different types of values (calorimetric, emf or vapor pressure, phase diagram measurements) have their special equations of error. Also for one type of measurement special equations exist for different number of phases [Zimmerman].

Zimmermann defines the error of a two-phase equilibrium by a linear expression relating the Gibbs energies and their derivatives with respect to the composition x as

$$G' + (x\text{-x}')\cdot\frac{\text{dG}'}{\text{dx}'}\text{-G} = 0 \qquad (2.70)$$

The first two terms together give the distance between this point at x' on the tangent to the curve G'(x) at x'. All three terms together thus give the distance between this point on the tangent and G" = G^{liq} at x" =x^{liq}. If the single-phase Gibbs energies are linear functions of the adjustable coefficients, the error itself is a linear adjustable coefficients. The thus-defined error is zero if the common-tangent construction fits exactly with the measured concentration x'.

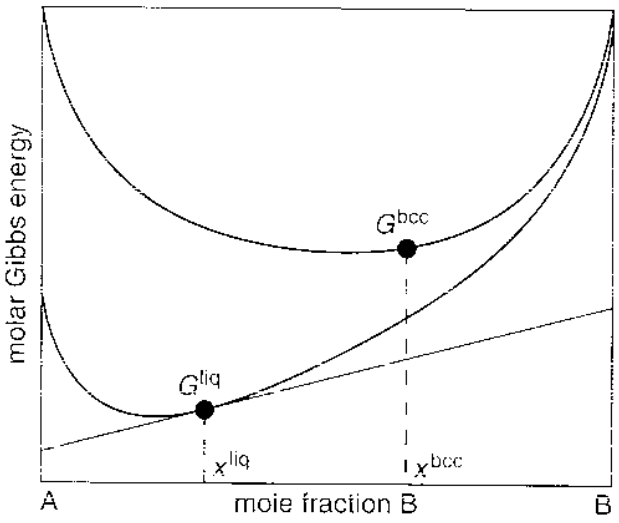

Fig 2.16. Construction of the 'alternate definition of error'. The difference taken at composition x^{bcc} between G^{bcc} and the tangent touching G^{liq} at x^{liq} is taken to be the "error".

The general equations of our problem are outlined as follows:

The minimum of the sum of the squares of errors is determined by the method of Gauss, which can be expressed in matrix formulation. The corrections of the coefficients are the solutions of the matrix equation.

A set of n measurable values W_i depends on a set of m unknown coefficients V_i via functions F_i with values of independent variables x_{ki}:

$$W_i=F_i(V_j, x_{ki}) \qquad i=1,\ldots,n, \quad j=1,\ldots\ldots,m \qquad (2.71)$$

The index k distinguishes the various independent variables (temperature, concentrations …) belonging to measurement number i.

If n is greater than m it is not possible to find the set of coefficients V_j for which the W_i calculated are equal to the corresponding measured values L_i. The best values of V_j obtained which minimizes the sum of the squares of errors, error is defined as the difference between calculated and measured F_i and L_i values times the weighing factor p_i:

$$(F_i(V_j,x_{ki})-L_i)\cdot p_i = v_i \quad \text{equation number} \tag{2.72}$$

p_i is called the error equation.

The condition for the best value of $V_{j\ with}$ respect to V_j is

$$\sum_{i=1}^{n} v_i{}^2 = min \tag{2.73}$$

The derivation of the above m equations with respect to *m* unknown coefficients V_j is written as

$$\sum_{i=1}^{n} v_i \cdot \frac{\partial v_i}{\partial C_j} = 0$$

$$j = 1,\ldots,m \tag{2.74}$$

Linear expansion of v_i in terms of Taylor series

$$v_i\left(V_j,x_{ki}\right) \approx v_i^0\left(V_j^0,x_{ki}\right) + \sum_{l=1}^{m} \frac{\partial v_i}{\partial V_l} \cdot \Delta V_l \tag{2.75}$$

Where the ΔV_i are the corrections to the coefficients V_i. if the difference between V_j^0 values and the final values are too high which is invalid which are non-linear in the coefficients V_j. The corrections can be calculated by inserting the Eq. 2.75 into Eq. 2.74 and rearranging to give:

$$\sum_{l=1}^{m}\left(\sum_{l=1}^{n}\frac{\partial v_i}{\partial V_j}\cdot\frac{\partial v_i}{\partial V_l}\right)\Delta V_i = -\sum_{i=1}^{n} v_i^0\cdot\frac{\partial v_i}{\partial V_j} \quad j=1,\dots,m \tag{2.76}$$

These are called "Gaussian normal equations" with *m* set of linear equations for the *m* unknowns:

$$\left(\left(\sum_{i=1}^{n}\frac{\partial v_i}{\partial V_j}\cdot\frac{\partial v_i}{\partial V_l}\right)\right)_{m,m}(\Delta V_l)_{m,1} = \left(\left(-\sum_{i=1}^{n} v_i^0\cdot\frac{\partial v_i}{\partial V_j}\right)\right)_{m,1} \quad j=1,\dots,m \tag{2.77}$$

Set of coefficients initial coefficients ΔL_i^0 when incorporated in the above set of Eq (6.7) solves the corrections ΔV_i . Until the corrections are less than the given limit, the corrections are being added to the initial set of coefficients and checked.

The mean square error is defined as a measure of the fit between the measured values and the resulting V_j :

$$mean\ square\ of\ error = \sum_{i=1}^{n}\frac{v_i^2}{n-m} \tag{2.78}$$

So the accuracy of the calculate coefficients is proportional to the square root of the mean squared error. The factor of proportionality of each coefficient is the square root of the corresponding diagonal element of the reciprocal of the *m x m* matrix of Eq.(2.77)

The squares of errors in Eq (2.73) should have the same dimension. The weighing factor p_i in Eq (2.72) can be used to make the errors v_i dimensionless, if p_i is taken as the reciprocal of the estimated accuracy ΔL_i of the measured values [2]:

$$p_{i=(\Delta L_i)^{-1}} \tag{2.79}$$

In PARROT software the term sum of squares of errors for each experimental value *i* is equal to $\left(weight_i \cdot \frac{(experimental\ value)_i - (calculated\ value)_i}{(estimated\ uncertainty)_i}\right)^2$ (2.80)

This equation is equivalent to the addition of Eqs (2.72) and (2.79) without considering the uncertainties of the independent variables.

2.7. PARROT module of THERMO-CALC

2.7.1 .The PARROT Program

The PARROT program which is integrated into the Thermo-Calc software is the tool to perform optimization. The principle behind the program is to minimize the error between the experimental and the calculated quantities. PARROT separates the data in to independent and dependent variables in order to best-fit the model parameters. Any kind of model parameter can be optimized, including magnetic and pressure-dependent parameters, in all models that have been implemented in the Gibbs Energy System (GES), which is also a part of Thermo-Calc. PARROT gives all the possible information regarding the system to be assessed. PARROT has another important module EDIT-

EXPERIMENT for manipulating the optimizing conditions and individual experimental equilibrium. For example,

ENTER-PARAM L (LIQUID, AU, CU; 0) 298.15 V1+V2*T; 6000 N

Also the Gibbs energies of the systems can be functions of temperature and pressure with several parameters to be optimized.

In the PARROT module of Thermo-Calc there is no limitation in definition the error for each experiment, thus the alternate definition can be chosen independently. The PARROT module has an option called "set alternate mode," with the use of which alternate errors can be calculated from a 'normal' experimental data file as differences of Gibbs energies rather than differences between the measured and calculated quantity.

All the possible information related to the system to be assessed can be given to the program from the keyboard. The optimization is stated by creating the text files for data and commands, the most important files are the *setup file* and the *experimental data file*.

Optimization procedure:

Inaccuracies in experimental conditions can be taken into account in two ways in PARROT:

1. The inaccuracies in conditions, i.e., independent state variables, can be prescribed in the POLY-3 interface. In this case an equilibrium will be calculated with the experimental values of independent state variables. The standard deviations of the dependent state variables will be calculated by use of the error-propagation law,

presuming linear dependences of the dependent state variable on the independent state variables.

2. The “true” value of the condition can be optimized by using one of the defined variables as the condition. This can be obtained by the IMPORT command in the experimental data file. In this case the experimental observations of the independent state variable should be specified in the EXPERIMENT command in the experimental data file. The commands that can be used in the experimental data file are a subset of the commands available in the POLY-3 module, with a few extensions.

Both methods can be transformed to the problem of finding the minimum of the sum of squares. Method 2 can be used when several experiments have been performed under the same, badly determined, conditions. The two methods can be mixed in the same optimization run.

The set of adjustable coefficients, in PARROT called variables, that give a minimum of the sum of squares is found by numerical subroutine called VA05A from Harwell subroutine Library.

2.7.2. Optimization with PARROT [2]

The assessor should prepare the following files during assessment. These are briefly described as follows

POP file with experimental data,
SETUP file with models and known and unknown parameters,

EXP file with experimental data to be plotted, and

MACRO files for quick calculation of various diagrams.

A simple description of the flow of assessment work would be as follows

1. Preparation of the SETUP and POP and EXP files with a text editor
2. Starting PARROT and run the SETUP file once to create the work file, usually called the PAR file since its extension is ".PAR." The PAR file is machine-dependent and cannot be read by a text editor. It can be manipulated only through the PARROT module. The PAR file will always contain the last results and is automatically updated whenever it is used in PARROT. Whenever a user wants to "freeze" a reasonable set of model parameters but perhaps continue trying to change the weightings or set of model parameters, it is advisable to make a copy of PAR file.
3. COMPILE the POP file inside the PARROT module. The experimental data will be stored on the PAR FILE.
4. Selection of variables to be optimized.
5. SET-ALTERNATE-MODE ON and optimize all equilibria until they have converged.
6. RESCALE the variables to set the start values to the final values.
7. Optimize and rescale until no more changes occur.
8. SET-ALTERNATE-MODE OFF.
9. Calculating of diagrams and comparing the results with experimental data. This should be done whenever needed during the steps below also. The sum of errors is

not a sufficient measure of the overall fit. We may find it convenient to make MACRO files to calculate several diagrams.

10. Use the EDIT-EXPERIMENT module to COMPUTE-ALL equilibria. Some equilibria might not converge or may converge to results far away from the experimental data. Some hints on how to handle that are given below. Experimental data that cannot be calculated should have SET-WEIGHT zero. SAVE when finished with the EDIT module.
11. Optimizing the variable zero times and checking the errors carefully, using the LIST-RESULT command. This output gives an overview of the current fit to all experimental data. We may have to use the EDIT module again to correct or remove (SET-WEIGHT) some equilibria.
12. Optimize and rescale the variable until the calculation has converged. We may find that some variable becomes very large or very small. That may be due to a lack of experimental information. We may have to increase or decrease the number of optimized variables and also use the EDIT module to select the weightings of the various experimental equilibria until we get reasonable results.
13. We may have to optimize “in parts” keeping the variables for some phases fixed and optimizing others with respect to selected sets of experimental data. The selections of experiments are made in the EDIT module.
14. We may have to iterate several times through all points above, even editing the POP and SETUP files, before we are satisfied. We can try various models for the phases and various numbers of variables for each phase.

15. A final optimization with all variables and all experiments with their selected weightings should be carried out.
16. Writing the report. When we do this, we may find that we cannot explain some decisions made during the optimization; and you may have to go back to optimize and try various new options.

The experimental data file, POP file

The experimental data on a system, taken from the literature or measured by the assessor, should be written onto a file called a "POP" file because of the default extension .POP. The experimental equilibria and measurements are described with POLY commands, with some additional features. The commands that are legal in a POP file are described in a special section of the POLY manual. It is very important to understand the state-flexible variable notation used in POLY and PARROT.

The POP file is a very important form of documentation because it describes the known experimental data for a system. The POP file is intended to be self documenting and readable both to a human and to the computer. The experimental data are described independently of the models selected for the phases. It is thus possible to use the same POP file to assess a system using different models for the phases. It is not uncommon that a system must be reassessed some years later when new information is available, or if a model for a phase should be changed. Since the reassessment may be done by someone other than the person who created the POP file, it is important that the information in the POP file is well organized and documented.

The result of an optimization must be checked by comparing all experimental data with the corresponding values calculated using the optimized dataset. This is usually done by plotting diagrams.

Output and Checking

It is difficult to know when the best possible set of parameters has been reached. The solution will depend on the best fit of optimized diagram with the experimental data points. The sub-regular model parameters L_0 of temperature-independent and L_1 of temperature-dependent are the only once to be optimized and these can be related to enthalpies and entropies, respectively. One may reset or discard the parameter values that are unreasonable for the reasons one should have. If the heat-capacity have been asses, the enthalpy and entropy must be recalculated from the Gibbs-energy expression and cannot just consider only the L_0 and L_1.

A well optimized set of parameters for the Gibbs energies of the system should be able to reproduce the available experimental set in one of the best possible following ways:

1. The final results and final errors of each measurement are printed in an additional file during the run of the program. The calculated coefficients can be incorporated in the excess terms of Gibbs energy equations and run in Thermo-Calc to post the phase diagram so as to get a visual check of the agreement between for experimental data and calculated data in the phase diagram.
2. Another point one can observe while optimizing is the term sum of the squares of errors obtained from the least-squares fit.

3. Extrapolating to higher order systems sometimes shows how successful is the description of the system.
4. If the value of the parameter of L_1 term is very large, that should be taken as an indication that L_0 and L_1 cannot be optimized independently and the constraint proposed by Tanaka et al. (1990) should be considered an adequate estimate.
5. Truncation of the non-significant digits in a parameter. Safe method of rounding of the digits must be followed.
6. Check that S_{298} and C_p of all the phases are within reasonable limit.

The principle of least squares method is to select the best match of all the experimental values and all the coefficients. Many of the coefficients of the descriptions, however, are not able to improve the fit between measurements and the descriptions significantly.

2.8. Thermodynamic Database and Importance of its Development

Using CALPHAD method, the functions relating the composition, temperature, pressure, Gibbs free energy for all the stable phases of a given system are used in construction and development of thermodynamic databases. The availability of these functions allows the calculation of multi-phase, multi-component equilibria at any temperature, composition, and pressure by the minimization of the total Gibbs energy for given conditions. Acquiring the equilibrium data for the metastable phases from the experimental data available is quite difficult, so good theoretical models are required to extrapolate data into the metastable phase regions.

Substance database

The substance databases have complex data of combined stoichiometric phases and gaseous components. It has more than 10.000 different substances so the difficulty arise in using this database is while getting the Gibbs energy data for a reaction individual constituents need to be specified clearly. Substance database doesn't have the difficulties with non-ideal mixing of substances.

Solution database

This considers the thermodynamic descriptions for phases in wide ranges of temperature and pressure. Miscibility gaps can appear ternary and higher order systems; the Gibbs phase rule helps in understanding such type of reactions. This may lead to the validation of the database for multi-component systems.

The continued developments in CALPHAD assessment of alloy and other materials phase diagrams was assisted by the creation of thermo chemical databanks. The advent of the computer provided a perfect platform for automating the storage and retrieval as well as the assessment and application of thermodynamic data. The availability of assessed parameters for many systems also allowed easy exchange and use of data by others in the field, thereby providing a basis for calculations and continuous addition and updating of the stored parameters.

The ongoing thermodynamic databank activities by members of communities like SGTE, Ecole Polytechnique in Montreal, KTH Stockholm, and NPL at AEA Harwell in UK, at University of Grenoble and IRSID, RWTH in Aachen Germany establish a common

databank accessible to all participants, provide an up-to-date data for the research activities.

All the above organizations contributed greatly to a dramatic increase in development of new materials with the use of thermodynamic calculations.

2.9. References

[1] Zi-kui-liu, *First Principle Calculations and Calphad modeling*, (2009)

[2] Hans Leo Lukas, Suzana G.Fries, Bo Sundman. *Computational Thermodynamics;Calphad method*

[3] N. Saunders, A.P. Miodownik, *CALPHAD – A Comprehensive Guide*, Pergamon Materials Series, 1998, Elsevier Science Limited, United Kingdom.

[4] M. Margules, *Sitzb. d. mathem.-nature*. C1.,CIV.Bd., Abth., II.a., 104, 1243

[5] O. Redlich and A. Kister *Ind. Eng. Chem.* 40, 345 (1948)

[6] J. D. Edsaile. *Metall. Trans*. 2, 2277 (1971)

[7] R.L Sharkey. M. J. Pool and M. Hoch, *Metall. Trans*. 2 3039 (1971)

[8] C. W. Bale and A.D. Pelton. *Metall.trans.* 5, 2323 (1974)

[9] J. Tomiska. *Calphad*. 10, 1, 91 (1986)

[10] J.J. Van Laar. *J. Phy.Chem*. 83 215 (1942)

[11] G. Scatchard and W. J. Hamer. *J. Amer. Chem. Soc.* 7 1805 (1935)

[12] P.J. Flory. *J. Chem. Phys*. 10 51 (1942)

[13] M.L Huggins. *Ann. N.Y. Acad. Sci*. 43 1 (1942)

[14] K. Wohl. *Trans. Am. Inst. Chem. Eng*. 42 215 (1946)

[15] G.M. Wilson. *J. Amer. Chem. Soc*. 86 127 (1964)

[16] I. Ansara *pure & App. Chem.,* Vol.70, No. 2, pp. 449-459, 1998

[17] Matts Hillert *Thermodynamics and Phase Transitions*

[18] Robert T. DeHoff *Thermodynamics in materials science*

[19] *Introduction to Metallurgical Thermodynamics* By David Gaskell

[20] Jansson, B.; Schalin, M.; Sundman, B, *J.Phase Equilibria* (1993) 14(5), 557-62

[21] H.L Lukas, Henig, E.T Zimmermann, B. *CALPHAD* (1977), 1(3), 225-36.

[22] K.C. Hari Kumar, 1999, Dept. MTM, Katholieke Universiteit Leuven, Belgium

CHAPTER 3

Results and Discussion

3.1. Thermodynamic Computations

Calculation of TRIS-AMPL binary phase diagram, exhibiting two phase region ODIC phases (FCC-BCC), referred to as non-isomorphous systems

This section involves the general aspects of our modeling strategy using TRIS as A system that can be extended to AMPL as B. Computational method such as Calphad is employed to model thermodynamic properties for each phase. Pure Gibbs energies of different phases are adequate to use regular-solution model. We adopted the standardized nomenclature for various phases, prior work by Chandra et al. denoted α or β to be the lower temperature phase and γ or γ' prime to be the higher temperature plastic phases and the liquid phase L. Now we have to model the Gibbs energies of solutions phases φ(φ=α, β, γ, γ, L). If the reference state for each phase is taken to be that of the pure components in that phase, then the Gibbs energy of a solution phase φ(φ=α, β, γ, γ, L) can be represented as follows(units of Gibbs energy throughout this work, where a mol is a mole of formula unit):

$$G^{\Phi} = x_A{}^{\circ}G_A^{\Phi} + x_B{}^{\circ}G_B^{\Phi} + RT[x_A \ln(x_A) + x_B \ln(x_B)] + G^{EX,\Phi} \quad (1)$$

Where, Φ= α, β, γ, γ1, L, R= 8.314 J $mol^{-1}K^{-1}$, x_A is mole fraction of 'A' and x_B is the mole fraction of 'B'. ${}^{\circ}G_A^{\Phi}$ and ${}^{\circ}G_B^{\Phi}$ same as Φ. We choose a single reference phase for each component and express the pure component Gibbs energies in Φ.

$$G^{EX,\Phi} = x_A x_B\left(L_0^{\Phi} + L_1^{\Phi}(x_A - x_B)\right) \quad (2)$$

L_0^{Φ} and L_1^{Φ} are the excess Gibbs energy parameters.

For a phase Φ(Φ=α,β,γ,γ',L), $^{\circ}G_A^{\Phi}$ and $^{\circ}G_B^{\Phi}$ are the reference states of pure 'A' and 'B', same as . We chose a single reference phase for each component and express the pure component Gibbs energies of other phases as changes from this reference phase. We chose al phase for A and be phase for 'B' and set them equal to zero to get $^{\circ}G_A^{\alpha} = 0$ and $^{\circ}G_B^{\beta}$=0

The stable phases for 'A' are α and γ and β and γ' for 'B'. Gibbs energies of the other phases in terms of these reference states can be represented as:

$$^{\circ}G_A^{\gamma} = {}^{\circ}G_A^{\alpha} + \Delta\text{--}{}^{\circ}G_A^{\alpha\to\gamma} = \Delta{}^{\circ}G_A^{\alpha\to\gamma} \quad (3)$$

$$^{\circ}G_A^{L} = {}^{\circ}G_A^{\alpha} + \Delta{}^{\circ}G_A^{\alpha\to L} = \Delta\text{--}{}^{\circ}G_A^{\alpha\to\gamma} + \Delta{}^{\circ}G_A^{\gamma\to L} \quad (4)$$

$$^{\circ}G_B^{\gamma'} = {}^{\circ}G_B^{\beta} + \Delta{}^{\circ}G_B^{\beta\to\gamma'} = \Delta{}^{\circ}G_B^{\alpha\to\gamma'} \quad (4)$$

$$^{\circ}G_B^{L} = {}^{\circ}G_B^{\beta} + \Delta{}^{\circ}G_B^{\beta\to L} = \Delta{}^{\circ}G_B^{\beta\to\gamma'} + \Delta{}^{\circ}G_B^{\gamma'\to L} \quad (6)$$

The pure component stable Gibbs energies, $^{\circ}G_A^{\alpha}$, $^{\circ}G_A^{\gamma'}$, $^{\circ}G_A^{\beta}$, $^{\circ}G_A^{\gamma}$ were determined including the heat capacity data. The following are the Gibbs energies of the stable phases of component:

$$^{\circ}G_A^{\gamma} = \Delta{}^{\circ}G_A^{\alpha\to\gamma} = \Delta H_{TR} - T\Delta S_{TR} + \int_{T_{TR}}^{T}\Delta C_P^{\alpha\to\gamma} - T\int_{T_{TR}}^{T}\frac{\Delta C_P^{\alpha\to\gamma}}{T}dT \quad (7)$$

$$^{\circ}G_A^L = \Delta^{\circ}G_A^{\alpha\to\gamma} + \Delta^{\circ}G_A^{\gamma\to L} = \Delta H_{TR} - T\Delta S_{TR} + \int_{T_{TR}}^{T} \Delta C_P^{\alpha\to\gamma} - T\int_{T_{TR}}^{T} \frac{\Delta C_P^{\alpha\to\gamma}}{T} dT$$

$$+\Delta H_F - T\Delta S_F + \int_{T_{TR}}^{T} \Delta C_P^{\alpha\to\gamma} - T\int_{T_{TR}}^{T} \frac{\Delta C_P^{\alpha\to\gamma}}{T} dT \quad (8)$$

Similarly expressions can be drawn for Gibbs energies for stable phases of 'B' using Eqs (6) and (7)

The metastable Gibbs energies can be estimated from these Gibbs energies. For example, for 'A' in be phase, the difference, G-G is needed such that we express

$$^{\circ}G_A^{\beta} = {}^{\circ}G_A^{\alpha} + M_A^{\beta} \quad (9)$$

The Gibbs energy of β phase, G_m^{β} can be written as

$$G_m^{\beta} = x_A\left({}^{\circ}G_A^{\alpha} + M_A^{\beta}\right) + x_B{}^{\circ}G_B^{\beta} + RT[x_A\ \ln(x_A) + x_B\ \ln(x_B)] + G^{EX,\beta} \quad (10)$$

$$= x_A\, M_A^{\beta} + RT[x_A \ln(x_A) + x_B \ln(x_B)] + G^{EX,\beta} \quad (11)$$

Similarly for the α phase, we can write the Gibbs energy, G_m^{α}, as:

$$G_m^{\alpha} = x_A{}^{\circ}G_A^{\alpha} + x_B\left({}^{\circ}G_B^{\beta} + M_A^{\alpha}\right) + RT[x_A\ \ln(x_A) + x_B\ \ln(x_B)] + G^{EX,\alpha} \quad (12)$$

$$= x_B\, M_B^{\alpha} + RT[x_A \ln(x_A) + x_B \ln(x_B)] + G^{EX,\alpha} \quad (13)$$

To estimate M_A^{β} and M_B^{α}, we assume that α and β phases are ideal solutions.

Therefore, the partial molar Gibbs energies can be written as [5]:

$$\bar{G}_B^{\beta} = {}^{\circ}G_B^{\beta} + RTln\,(x_B^{\beta}) \tag{14}$$

$$\bar{G}_B^{\alpha} = {}^{\circ}G_B^{\alpha} + RTln\,(x_B^{\alpha}) \tag{15}$$

Where, $\bar{G}_B^{\beta}$ and $\bar{G}_B^{\alpha}$ are the partial molar Gibbs energies of 'B' in β and α phases respectively. At equilibrium, $\bar{G}_B^{\beta} = \bar{G}_B^{\alpha}$, we can make the following estimation at the temperature of maximum solubility, $T=T_{max}$,

$$ {}^{\circ}G_B^{\alpha} = G_B^{\beta} + RT_{max} \ln\left(\frac{x_{B\,\max}^{\beta}}{x_{B\,max}^{\alpha}}\right) = RT_{max} ln\left(\frac{x_{B\,\max}^{\beta}}{x_{B\,max}^{\alpha}}\right) \tag{16}$$

$$M_B^{\alpha} = 8.314 \times 345 \times ln\left(\frac{0.86}{0.15}\right) = 5008.9\ J\ mol^{-1}$$

A similar expression can be made for M_A^{β} and is given by,

$$ {}^{\circ}G_A^{\beta} = {}^{\circ}G_A^{\alpha} + RT_{max} \ln\left(\frac{x_{A\,\max}^{\beta}}{x_{A\,max}^{\alpha}}\right) = RT_{max} ln\left(\frac{x_{A\,\max}^{\beta}}{x_{A\,max}^{\alpha}}\right) \tag{17}$$

$$M_B^{\alpha} = 8.314 \times 345 \times \left(\frac{0.85}{0.14}\right) = 5173.3\ J\ mol^{-1}$$

The assumption that α and β phases are ideal solutions is used only to describe the metastable pure Gibbs energies ${}^{\circ}G_B^{\alpha}$ and ${}^{\circ}G_A^{\beta}$. The nature of non-ideality of the α phase can still be expressed using sun-regular solution model for $G^{EX,\alpha}$

To estimate the metastable $^{\circ}G_B^{\alpha}$and $^{\circ}G_A^{\beta}$, we again assume ideal solutions and thus we can make the following estimations:

$$^{\circ}G_A^{\gamma\prime} = {}^{\circ}G_A^{\gamma\prime} + RT_{max}\ln\left(\frac{x_{A\,\max}^{\gamma}}{x_{A\,max}^{\gamma\prime}}\right) = \Delta^{\circ}G_A^{\alpha\rightarrow\gamma} + RT_{max}\ln\left(\frac{x_{A\,\max}^{\gamma}}{x_{A\,max}^{\gamma\prime}}\right) \quad (18)$$

$$M_A^{\gamma\prime} = RT_{max}\ln\left(\frac{x_{A\,\max}^{\gamma}}{x_{A\,max}^{\gamma\prime}}\right) = 8.314 \times ln\left(\frac{0.6}{0.4}\right)$$

The above calculations were shown in the following Math-cad files in detail.

3.1.1. Gibbs energy calculations

A – AMPI

α – γ

$\Delta H_{TR\_\gamma} := 2345($

$\Delta S_{TR\_\gamma} := 66.0$

$T_{TR} := 353$

$\Delta H_{F\_\gamma} := 2991.$

$\Delta S_{F\_\gamma} := 7.2$

B – TRIS

β – γ1

$\Delta H_{TR\_\gamma 1} := 3269($

$\Delta S_{TR\_\gamma 1} := 80.1$

$T_{TR2} := 40$

$\Delta H_{F\_\gamma 1} := 334($

$\Delta S_{F\_\gamma 1} := 7.50($

Since α and β is taken as reference state the corresponding Cp is zero

$C_{P\_\alpha}(T) := 0$

$C_{P\_\beta}(T) := 0$

$C_{P\_\gamma}(T) := 110 + 0.55 \cdot T$

$C_{P\_\gamma 1}(T) := 104.094 + 0.922 \cdot T$

$C_{P\_LA}(T) := 80 + 0.482 \cdot T$

$C_{P\_LB}(T) := 57.714 + 0.817 \cdot T$

$\Delta C_{P\_\alpha\gamma}(T) := C_{P\_\gamma 1}(T) - C_{P\_\alpha}(T)$

$\Delta C_{P\_\beta\gamma 1}(T) := C_{P\_\gamma}(T) - C_{P\_\beta}(T)$

$\Delta C_{P\_\alpha\gamma}(T) \rightarrow 104.094 + .922 \cdot T$

$\Delta C_{P\_\beta\gamma 1}(T) \rightarrow 110 + .55 \cdot T$

$$\Delta C_{P\_\gamma L}(T) \rightarrow (-24.094) - .440\,T \qquad \Delta C_{P\_\gamma 1L}(T) \rightarrow (-52.286) + .267\,T$$

$$G_{0\_B\_\gamma 1} := \Delta H_{TR\_\gamma 1} - T\cdot\Delta S_{TR\_\gamma 1} + \int_{T_{TR2}}^{T} \Delta C_{P\_\beta\gamma 1}(T)\,dT - T\cdot\int_{T_{TR2}}^{T} \frac{\Delta C_{P\_\beta\gamma 1}(T)}{T}\,dT$$

$$G_{0\_B\_\gamma 1} := -86520.256 + 23.974\,T + .461\cdot T^2 - .922\cdot T^2 - 104.094\,T\cdot\ln(T) + 1001.913\,T$$

$$G_{0\_B\_\gamma 1} \rightarrow (-86520.256) + 1025.887\,T - .461\cdot T^2 - 104.094\,T\cdot\ln(T)$$

$$K_B(T) := \left(\int_{T_{TR2}}^{T} \Delta C_{P\_\beta\gamma 1}(T)\, dT - T \cdot \int_{T_{TR2}}^{T} \frac{\Delta C_{P\_\beta\gamma 1}(T)}{T}\, dT \right)$$

$$K_B(T) := 104.094T + .461 \cdot T^2 - 119210.256 - .922 T^2 - 104.094T \cdot \ln(T) + 1001.912T$$

$$K_B(T) \rightarrow 1106.006T - .461 \cdot T^2 - 119210.256 - 104.094T \cdot \ln(T)$$

$$G_{0\_A\_\gamma} := \Delta H_{TR\_\gamma} - T \cdot \Delta S_{TR\_\gamma} + \int_{T_{TR}}^{T} \Delta C_{P\_\alpha\gamma}(T)\, dT - T \cdot \int_{T_{TR}}^{T} \frac{\Delta C_{P\_\alpha\gamma}(T)}{T}\, dT$$

$$G_{0\_A\_\gamma} := -49647.475 + 43.99T + .275 T^2 - .55 T^2 - 110 \cdot T \cdot \ln(T) + 839.461T$$

$$G_{0\_A\_\gamma}\text{expand, float, 7} \rightarrow \left[\left[(-49647.475) + 883.451T - .275 T^2 - 110 \cdot T \cdot \ln(T) \right] \cdot \text{expand, float, 7} \right]$$

$$T \cdot \Delta S_{TR\_\gamma} \rightarrow 66.01T \qquad T \cdot \Delta S_{TR\_\gamma 1} \rightarrow 80.12T$$

$$\left(\int_{T_{TR}}^{T} \Delta C_{P\_\alpha\gamma}(T)\, dT\right) \rightarrow 104.094000000000000\cdot T + .461000000000000000\cdot T^2 - 94189.9310000000000$$

$$T\cdot\int_{T_{TR}}^{T} \frac{\Delta C_{P\_\alpha\gamma}(T)}{T}\, dT \rightarrow T\cdot(.922000000000000000\cdot T + 104.094000000000000\cdot\ln(T) - 936.130125918414593)$$

$$\underset{\wedge\wedge\wedge\wedge}{K}(T) := .275T^2 + 110\cdot T - 73097.475 - .55T^2 - 110\cdot T\cdot\ln(T) + 839.461T$$

$$K(T) \rightarrow (-.275)\cdot T^2 + 949.461T - 73097.475 - 110\cdot T\cdot\ln(T)$$

$$G_{0\_A\_\gamma L} := \Delta H_{F\_\gamma} - T\cdot\Delta S_{F\_\gamma} + \int_{T_{F\_\gamma}}^{T} \Delta C_{P\_\gamma L}(T)\, dT - T\cdot\int_{T_{F\_\gamma}}^{T} \frac{\Delta C_{P\_\gamma L}(T)}{T}\, dT$$

$$G_{0\_A\_\gamma L} := 19581.05 - 37.77T - .34e\text{-}1\cdot T^2 + .68e\text{-}1\cdot T^2 + 30\cdot T\ln(T) - 204.777T$$

$$G_{0\_A\_\gamma L} \rightarrow 19581.05 - 242.547T + .34e\text{-}1 \cdot T^2 + 30 \cdot T \cdot \ln(T)$$

$$T \cdot \Delta S_{F\_\gamma} \rightarrow 7.24T$$

$$K_{GA\_L} := \int_{T_{F\_\gamma}}^{T} \Delta C_{P\_\gamma L}(T)\, dT - T \cdot \int_{T_{F\_\gamma}}^{T} \frac{\Delta C_{P\_\gamma L}(T)}{T}\, dT$$

$$K_{AL}(T) := K(T) - 30 \cdot T - .34e\text{-}1 \cdot T^2 + 16589.65 + .68e\text{-}1 \cdot T^2 + 30 \cdot T \cdot \ln(T) - 204.777T$$

$$K_{AL}(T) \rightarrow (-.241) \cdot T^2 + 714.684T - 56507.825 - 80 \cdot T \cdot \ln(T)$$

$$G_{0\_A\_L} := G_{0\_A\_\gamma} + G_{0\_A\_\gamma L}$$

$$G_{0\_A\_L} \rightarrow (-30066.425) + 640.904T - .241 \cdot T^2 - 80 \cdot T \cdot \ln(T)$$

$$G_{0\_A\_\gamma L} \rightarrow 19581.05 - 242.547T + .34e\text{-}1 \cdot T^2 + 30 \cdot T \cdot \ln(T)$$

$$T \cdot \Delta S_{F\_\gamma} \rightarrow 7.24 \cdot T$$

$$K_{GA\_L} := \int_{T_{F\_\gamma}}^{T} \Delta C_{P\_\gamma L}(T)\, dT - T \cdot \int_{T_{F\_\gamma}}^{T} \frac{\Delta C_{P\_\gamma L}(T)}{T}\, dT$$

$$K_{AL}(T) := K(T) - 30 \cdot T - .34e\text{-}1 \cdot T^2 + 16589.65 + .68e\text{-}1 \cdot T^2 + 30 \cdot T \cdot \ln(T) - 204.777T$$

$$K_{AL}(T) \rightarrow (-.241) \cdot T^2 + 714.684T - 56507.825 - 80 \cdot T \cdot \ln(T)$$

$$G_{0\_A\_L} := G_{0\_A\_\gamma} + G_{0\_A\_\gamma L}$$

$$G_{0\_A\_L} \rightarrow (-30066.425) + 640.904T - .241 \cdot T^2 - 80 \cdot T \cdot \ln(T)$$

$$G_{0\_B\_\gamma 1L} := \Delta H_{F\_\gamma 1} - T\cdot\Delta S_{F\_\gamma 1} + \int_{T_{F\_\gamma 1}}^{T} \Delta C_{P\_\gamma 1L}(T)\,dT - T\cdot\int_{T_{F\_\gamma 1}}^{T} \frac{\Delta C_{P\_\gamma 1L}(T)}{T}\,dT$$

$$G_{0\_B\_\gamma 1L} := 34375.4125 - 53.886T - .525e\text{-}1\cdot T^2 + 0.105T^2 + 46.38T\cdot\ln(T) - 329.553T$$

$$G_{0\_B\_L} := G_{0\_B\_\gamma 1} + G_{0\_B\_\gamma 1I}$$

$$G_{0\_B\_L} \rightarrow (-52144.8435 + 642.448T - .4085T^2 - 57.714T\cdot\ln(T)$$

$$T\cdot\Delta S_{F\_\gamma 1} \rightarrow 7.506T$$

$$K_{BL}(T) := K_B(T) + \left(\int_{T_{F\_\gamma 1}}^{T} \Delta C_{P\_\gamma 1L}(T)\,dT - T\cdot\int_{T_{F\_\gamma 1}}^{T} \frac{\Delta C_{P\_\gamma 1L}(T)}{T}\,dT \right)$$

$$K_{BL}(T) := 1059.626T - .5135T^2 - 88174.843 - 104.094T\cdot\ln(T) + .105T^2 + 46.38T\cdot\ln(T) - 329.553T$$

$$K_{BL}(T) \rightarrow 730.073T - .4085T^2 - 88174.843 - 57.714T\cdot\ln(T)$$

GIBBS FREE ENERGY- COMPOSTION (G - X) DIAGRAMS

$$G_{0\_A\_\alpha} := 0$$

$$G_{0\_B\_\beta} := 0$$

$$G_{0\_B\_\alpha} := 5008.9$$

$$G_{0\_A\_\beta} := 5173.3$$

$$G_{0\_A\_\gamma}(T) := -49647.4750 + 883.451T - .275T^2 - 110 \cdot T \cdot \ln(T)$$

$$G_{0\_B\_\gamma 1}(T) := -86520.256 + 1025.887T - .461T^2 - 104.094T \cdot \ln(T)$$

$$G_{0\_A\_L}(T) := -30066.425 + 640.90T - .241T^2 - 80 \cdot T \cdot \ln(T)$$

$$G_{0\_B\_L}(T) := -52144.8430 + 642.448T - .4085T^2 - 57.714T \cdot \ln(T)$$

$$G_{0\_B\_\gamma}(T) := G_{0\_B\_\gamma 1}(T) + 669$$

$$G_{EX\_\alpha} := 0$$

$$G_{EX\_\beta} := 0$$

$$G_{EX\_L} := 0$$

$$R := 8.314$$

$$G_{\alpha}(X_B, T) := G_{0\_A\_\alpha}\cdot(1 - X_B) + G_{0\_B\_\alpha}\cdot X_B + R\cdot T\cdot\left[(1 - X_B)\ln(1 - X_B) + X_B\cdot\ln(X_B)\right] \quad *$$

$$G_{\beta}(X_B, T) := G_{0\_A\_\beta}\cdot(1 - X_B) + G_{0\_B\_\beta}\cdot X_B + R\cdot T\cdot\left[(1 - X_B)\ln(1 - X_B) + X_B\cdot\ln(X_B)\right] \quad *$$

$$G_{\gamma}(X_B, T) := G_{0\_A\_\gamma}(T)\cdot(1 - X_B) + G_{0\_B\_\gamma}(T)\cdot X_B + R\cdot T\cdot\left[(1 - X_B)\cdot\ln(1 - X_B) + X_B\cdot\ln(X_B)\right]$$

$$G_{\gamma 1}(X_B, T) := G_{0\_A\_\gamma 1}(T)\cdot(1 - X_B) + G_{0\_B\_\gamma 1}(T)\cdot X_B + R\cdot T\cdot\left[(1 - X_B)\cdot\ln(1 - X_B) + X_B\cdot\ln(X_B)\right]$$

$$G_{L}(X_B, T) := G_{0\_A\_L}(T)\cdot(1 - X_B) + G_{0\_B\_L}(T)\cdot X_B + R\cdot T\cdot\left[(1 - X_B)\cdot\ln(1 - X_B) + X_B\cdot\ln(X_B)\right]$$

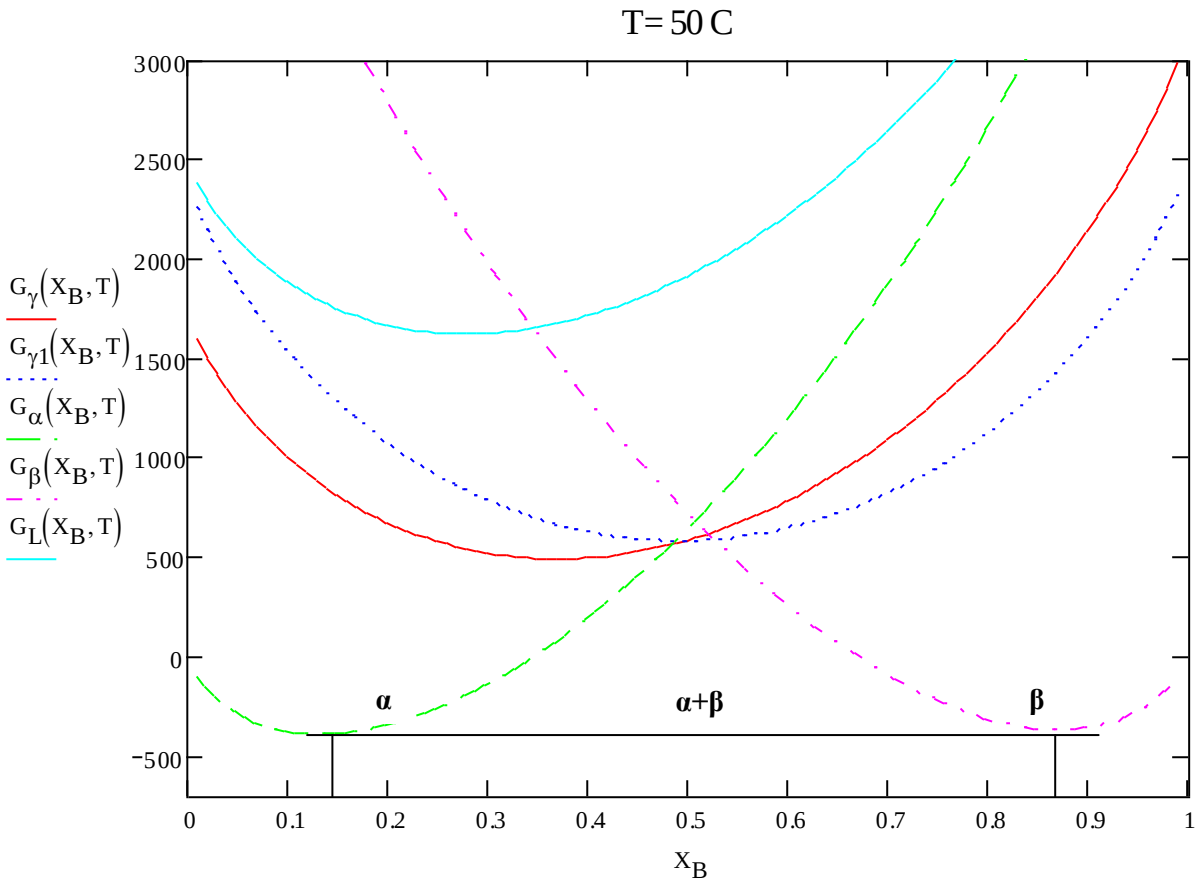
T= 50 C
$G_\gamma(X_B,T)$
$G_{\gamma 1}(X_B,T)$
$G_\alpha(X_B,T)$
$G_\beta(X_B,T)$
$G_L(X_B,T)$
3000
2500
2000
1500
1000
500
0
−500
α
α+β
β
0
0.1
0.2
0.3
0.4
0.5
0.6
0.7
0.8
0.9
1
X_B

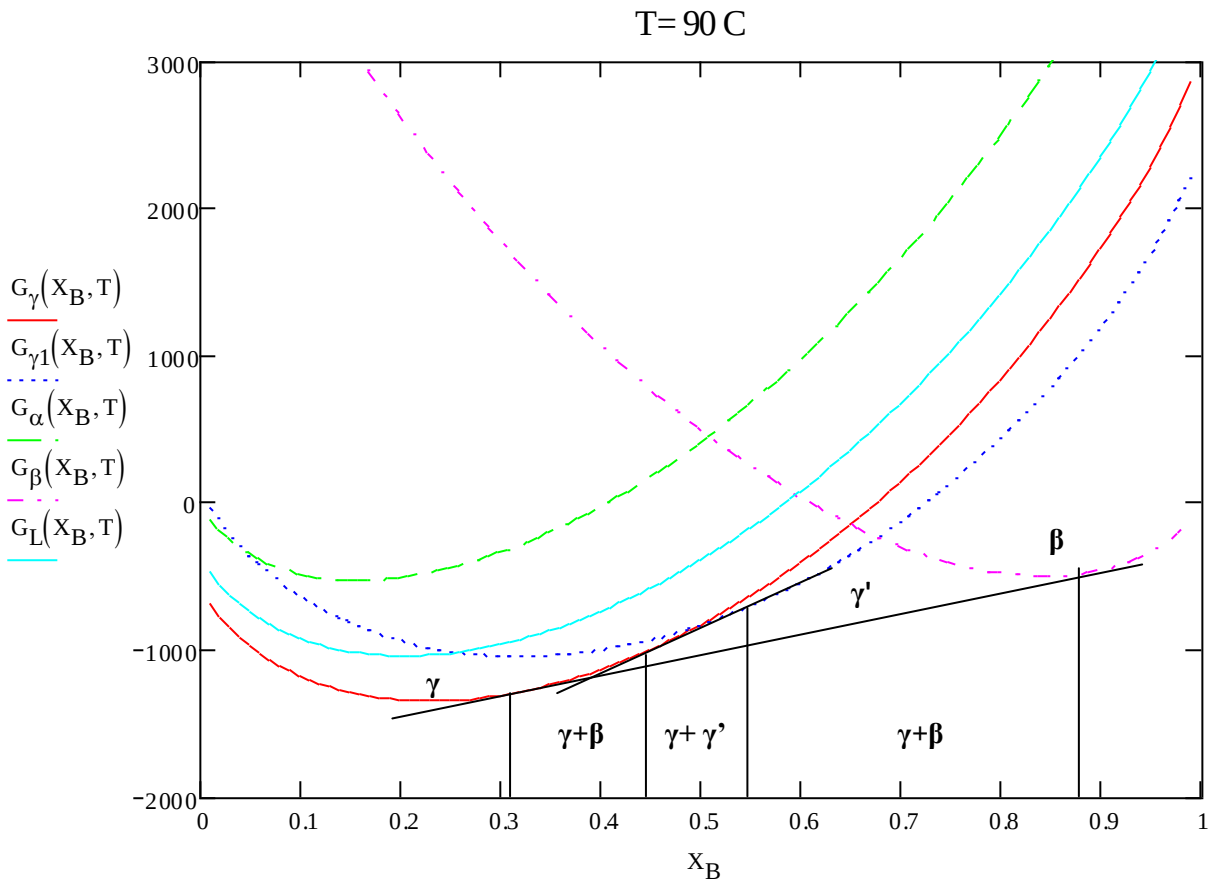
T= 90 C
$G_{\gamma}(X_B,T)$
$G_{\gamma 1}(X_B,T)$
$G_{\alpha}(X_B,T)$
$G_{\beta}(X_B,T)$
$G_L(X_B,T)$
3000
2000
1000
0
−1000
−2000
0
0.1
0.2
0.3
0.4
0.5
0.6
0.7
0.8
0.9
1
X_B
γ
γ+β
γ+ γ'
γ'
γ+β
β

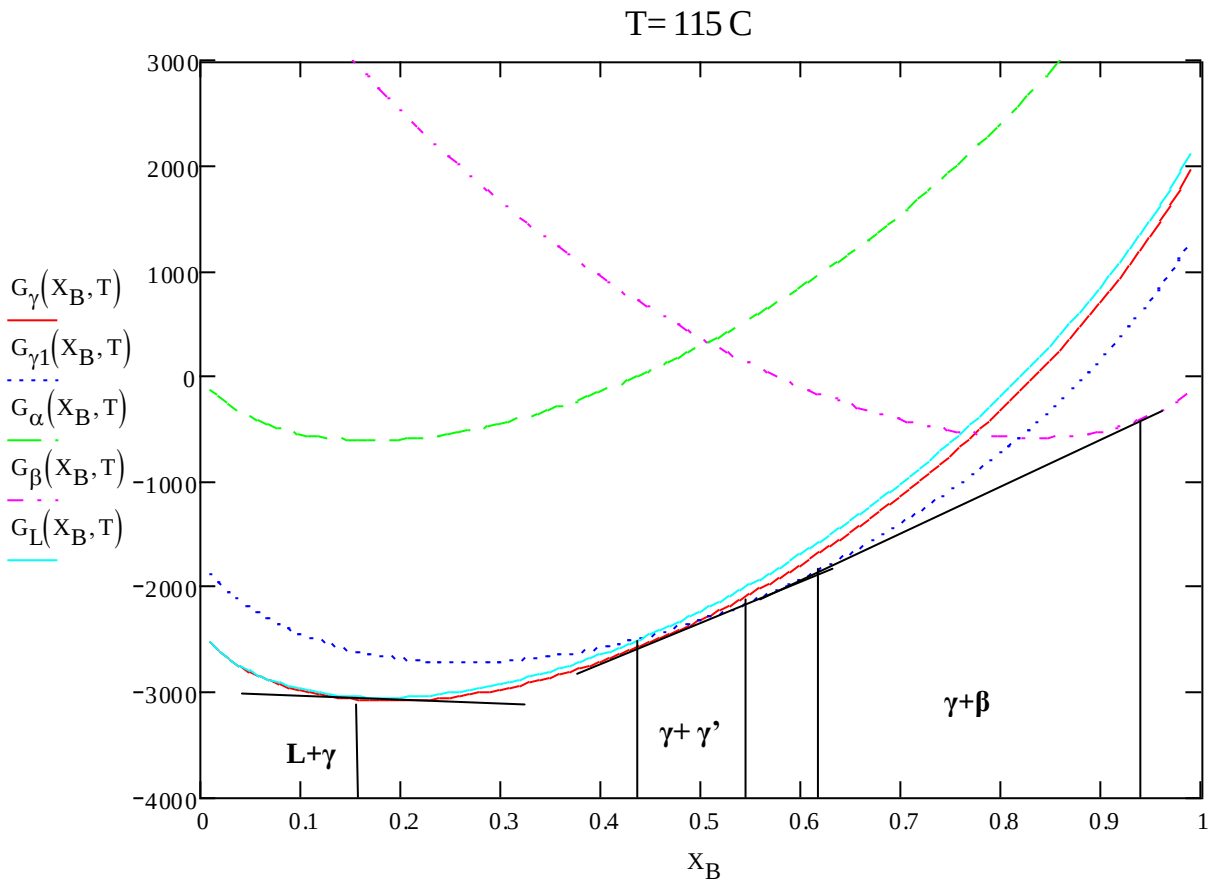
T= 115 C
$G_{\gamma}(X_B,T)$
$G_{\gamma 1}(X_B,T)$
$G_{\alpha}(X_B,T)$
$G_{\beta}(X_B,T)$
$G_L(X_B,T)$
3000
2000
1000
0
−1000
−2000
−3000
−4000
0
0.1
0.2
0.3
0.4
0.5
0.6
0.7
0.8
0.9
1
X_B
L+γ
γ+ γ'
γ+β

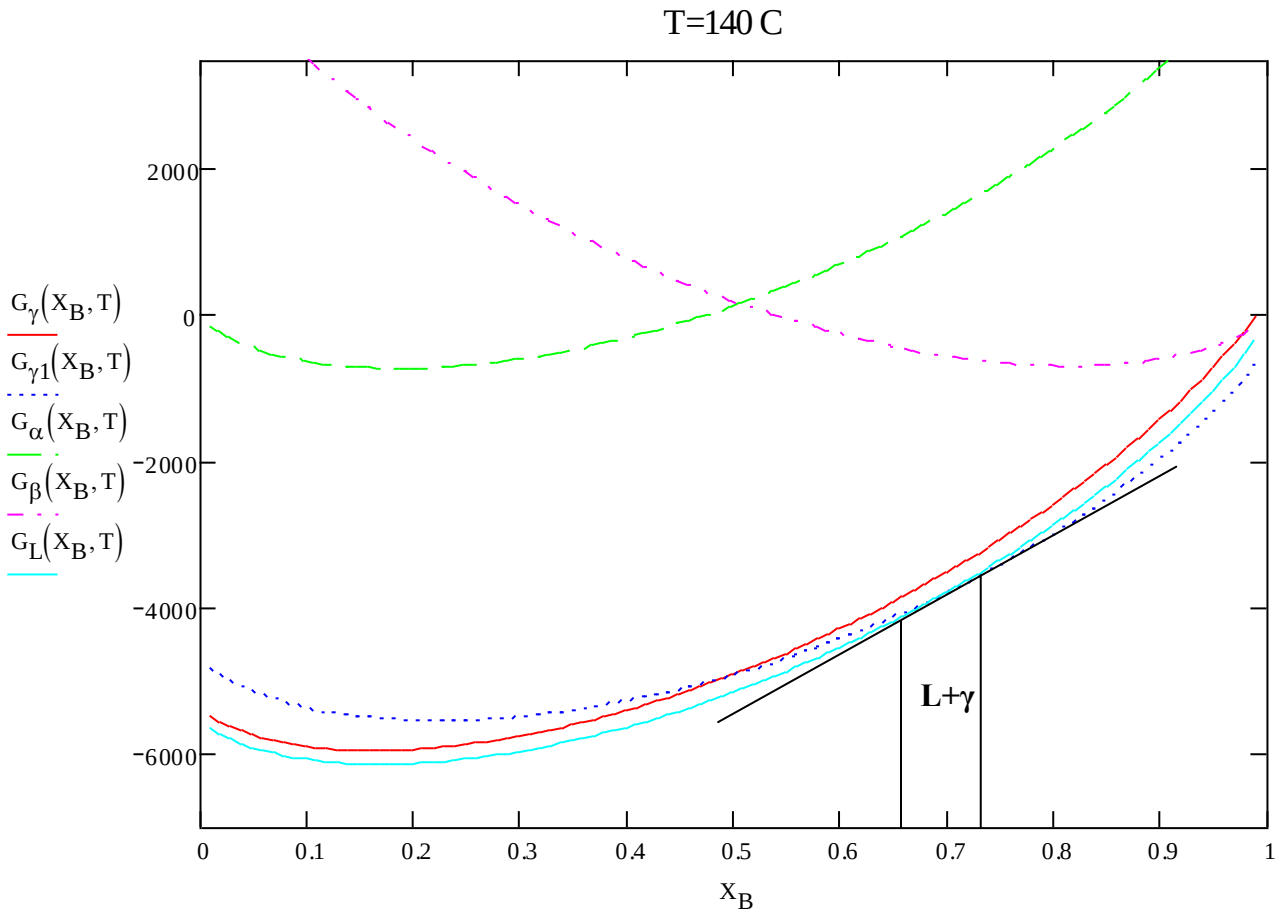
T=140 C
$G_\gamma(X_B,T)$
$G_{\gamma 1}(X_B,T)$
$G_\alpha(X_B,T)$
$G_\beta(X_B,T)$
$G_L(X_B,T)$
2000
0
-2000
-4000
-6000
0
0.1
0.2
0.3
0.4
0.5
0.6
0.7
0.8
0.9
1
X_B
L+γ

3.2. Experimental data for Optimization

Thermodynamic Properties of Pure AMPL and NPG

All previous phase diagram calculations [Barrio et.al] do not take into consideration any contribution from heat capacity to the Gibbs energy expressions for mathematical convenience. Inclusion of heat capacity expressions (Table 1) to calculate Gibbs energies (table 2), given in equations 3 to 6, results in non-linear dependence on temperature. An equation for Cp data for the γ' phase of pure AMPL was not available due to the small region between the solid-solid and solid-liquid transition temperature, but an approximation (interpolation between α and Liquid heat capacities) was made from our work Chandra et al.

Table 3.1. Crystal Structures, Transition Temperatures and Thermal properties of TRIS and AMPL [2].

Compound	**α or β Phases**	**T_{TR} (K)**	**ΔH_{TR} ($J.mol^{-1}$)**	**ΔS_{TR} ($J.mol^{-1}.K^{1}$)**	**γ' or γ Phases**	**T_F (K)**	**ΔH_F ($J.mol^{-1}$)**	**ΔS_{TR} ($J.mol^{-1}.K^{1}$)**
AMPL	Monoclinic	353	23540	66.01	BCC	385	2991	7.77
TRIS	Orthorhombic	408	32690	80.12	FCC	445	3340	7.32

3.3. Binary Phase Diagram data

The data that is available for these kinds of organic systems are essentially the tie lines and invariant equilibria determined by using DSC and X-ray diffraction. For the TRIS-AMPL system, there are no reported experimental data on activities or heat of mixing etc. in this work, we have only used the data from the works by Chandra et al.[2] for optimization. Chandra et al. [4] developed the experimental phase diagram of TRIS-AMPL in 2010, subsequently by Barrio et al.[1] in 1994. Although the global features of the phase diagram were reproduced in all the works [1, 4], there were some significant differences between them. Comparing the data of Barrio et al. and Chandra et al. Barrio expresses that there exists complete miscibility in the plastic phase implying that AMPL and TRIS have the same space group, where as Chandra et al showed the immiscibility existing in this region with by means of X-ray measurements. We use Chandra et al.[4] experimental data for optimization as we were unable to compromise such wide differences and moreover the useful temperature range for these organic binary phase diagrams is only 310K to 440K (solid and liquid phases).

Table 3.2. Heat Capacities of TRIS and AMPL [2].

Compound	**Heat Capacity Equations ($J.mol^{-1}.K^{-1}$)**	**Temperature Range**
AMPL	$CP(\alpha)=0$	305-322.5K
	$CP(\gamma')=110+0.55\cdot T$	327.5-337.5K
	$CP(L)=80+0.482\cdot T$	387.5-412.5K

TRIS	CP(β)=0	305-322.5K
	CP(γ)=104.094+0.922·T	327.5-387.5K
	CP(L)=57.714+0.817·T	430-440K

Note: since the chosen reference states are $°G_A^{\alpha} = 0$, and$G_B^{\beta} = 0$, the heat capacities Cp(α)=0 and C_p(β) =0 were used to determine stable and metastable modifications of pure component Gibbs energies.

3.4. Joback's method

Joback method is a group contribution method. The method predicts the thermodynamic properties for the most common functional groups using basic structural information of a chemical molecule like a list of simple functional groups.

The following table shows the group contribution for the non-ring groups, the Joback's method is being applied for the estimation of the thermodynamic data (enthalpy, entropy and Gibbs free energy) for the pure compounds AMPL and TRIS. Table 3 shows the Group contributions for different functional groups. The following calculations can be performed in MathCAD, a tool which can handle robust mathematical calculations.

Table 3.3.

Group Contributions

Group	T_c	P_c	V_c	T_b	T_m	H_{form}	G_{form}	a	b	c	d	H_{fusion}	H_{vap}	a	b
	Critical State Data			Temperatures of Phase Transitions		Chemical Caloric Properties		Ideal Gas Heat Capacities				Enthalpies of Phase Transitions		Dynamic Viscosity	
Non-ring groups															
-CH3	0.0141	-0.0012	65	23.58	-5.10	-76.45	-43.96	1.95E+1	-8.08E-3	1.53E-4	-9.67E-8	0.908	2.373	548.29	-1.719
-CH2-	0.0189	0.0000	56	22.88	11.27	-20.64	8.42	-9.09E-1	9.50E-2	-5.44E-5	1.19E-8	2.590	2.226	94.16	-0.199
>CH-	0.0164	0.0020	41	21.74	12.64	29.89	58.36	-2.30E+1	2.04E-1	-2.65E-4	1.20E-7	0.749	1.691	-322.15	1.187
>C<	0.0067	0.0043	27	18.25	46.43	82.23	116.02	-6.62E+1	4.27E-1	-6.41E-4	3.01E-7	-1.460	0.636	-573.56	2.307
=CH2	0.0113	-0.0028	56	18.18	-4.32	-9.630	3.77	2.36E+1	-3.81E-2	1.72E-4	-1.03E-7	-0.473	1.724	495.01	-1.539
=CH-	0.0129	-0.0006	46	24.96	8.73	37.97	48.53	-8.00	1.05E-1	-9.63E-5	3.56E-8	2.691	2.205	82.28	-0.242
=C<	0.0117	0.0011	38	24.14	11.14	83.99	92.36	-2.81E+1	2.08E-1	-3.06E-4	1.46E-7	3.063	2.138	n. a.	n. a.
=C=	0.0026	0.0028	36	26.15	17.78	142.14	136.70	2.74E+1	-5.57E-2	1.01E-4	-5.02E-8	4.720	2.661	n. a.	n. a.
≡CH	0.0027	-0.0008	46	9.20	-11.18	79.30	77.71	2.45E+1	-2.71E-2	1.11E-4	-6.78E-8	2.322	1.155	n. a.	n. a.
≡C-	0.0020	0.0016	37	27.38	64.32	115.51	109.82	7.87	2.01E-2	-8.33E-6	1.39E-9	4.151	3.302	n. a.	n. a.

AMPL STRUCTURE:

$(CH_3)(NH_2)-C-(CH2OH)_2 = C_4H_{11}O_2N$ Mol. Wt=105

$$\begin{pmatrix} \text{"2:-OH Non Ring"} \\ \text{"2:-CH2- Non Ring"} \\ \text{"1:>C< Non Ring"} \\ \text{"1:-CH3 Non Ring"} \\ \text{"1:-NH2 Non Ring"} \end{pmatrix} \quad \Delta H_{AMPL} := \begin{pmatrix} -208.4 \\ -20.64 \\ 82.23 \\ -76.45 \\ -22.02 \end{pmatrix} \quad \Delta G_{AMPL} := \begin{pmatrix} -189.20 \\ 8.42 \\ 116.02 \\ -43.96 \\ 14.07 \end{pmatrix}$$

$k := (2 \;\; 2 \;\; 1 \;\; 1 \;\; 1)$

$\Delta H_{0AMPLf} := 68.29 + k \cdot \Delta H_{AMPL}$

$\Delta H_{0AMPLf} \cdot 10^3 = -4.06 \times 10^5$

$\Delta G_{0AMPLf} := 53.88 + k \cdot \Delta G_{AMPL}$

$\Delta G_{0AMPLf} \cdot 10^3 = -2.216 \times 10^5$

$$S_{0AMPLf} := \frac{\left(\Delta H_{0AMPLf} - \Delta G_{0AMPLf}\right)}{298}$$

$S_{0AMPLf} \cdot 10^3 = -619.06$

TRIS STRUCTURE

$(NH_2)C\text{--}(CH_2OH)_3$ Mol wt=121

$$\begin{pmatrix} \text{"-NH2 Non Ring"} \\ \text{">C< Non Ring"} \\ \text{"-CH2- Non Ring"} \\ \text{"-OH Non Ring"} \end{pmatrix} \qquad \Delta H := \begin{pmatrix} -22.02 \\ 82.23 \\ -20.64 \\ -208.04 \end{pmatrix} \qquad \Delta G := \begin{pmatrix} 14.07 \\ 116.02 \\ 8.42 \\ -189.20 \end{pmatrix}$$

$k := (1 \;\; 1 \;\; 3 \;\; 3)$

$\Delta H_{0\_TRISf} := k \cdot \Delta H$

$\Delta G_{0\_TRISf} := k \cdot \Delta G$

$\Delta H_{0\_TRISf} 10^{3} = -6.258 \times 10^{5}$

$\Delta G_{0\_TRISf} 10^{3} = -4.122 \times 10^{5}$

$$S_{0TRISf} := \frac{\left(\Delta H_{0\_TRISf} - \Delta G_{0\_TRISf}\right)}{298}$$

$S_{0TRISf} 10^{3} = -716.711$

3.5. Results and Discussion

Phase diagram (unoptimized) and Effect of Heat Capacity

By using only pure enthalpies of the AMPL and TRIS compounds without having included any kind of experimental data shown in fig.1, estimated the temperature and composition range where the phase transitions can be formed, and then calculated the unoptimized phase diagram by including the calculated Gibbs energies for metastable phases. Simultaneously experiments can be conducted to determine to check for the accuracy of the temperature and composition conditions of phase transitions. Also calculated the phase diagram by adding Cp data to the Gibbs energy equations with the assumption of ideal solution phases, and observed the difference the phase diagram makes from the phase diagram without Cp data. The global features of the phase diagram are well represented in both the cases; with and without inclusion of Cp data to determine the Gibbs energies. But we can see from the Figure 2, that with the inclusion of Cp data to determined the Gibbs energies of the pure components, a significant improvement is achieved in the unoptimized phase diagram, especially in the invariant temperatures and compositions. There is a strong effect of Cp data especially for the low temperatures and compositions. There is a strong effect of Cp data especially for the low temperature eutectoid and the reason is due to the noticeable jump in Cp values during solid-solid transitions for TRIS and AMPL.

3.6. Optimized phase diagram for TRIS-AMPL Binary System

In order to determine the parameters for excess Gibbs energy, a thermodynamic optimization utilizing all available experimental data is desired. In this work, the following conditions for optimization were used:

i. It was assumed that $G^{EX,\alpha} = 0$ and $G^{EX,\beta} = 0$ because of limited miscibility.

ii. The high temperature γ' and γ phases were assumed to behave as sub regular solutions and the liquid phase was assumed to be ideal.

iii. No temperature dependency was assumed for all the excess parameters.

In parametric form, the excess Gibbs energies are of the following form:

For φ(φ=γ, γ'), $G^{EX\Phi,} = x_A x_B(L_0^{\Phi}+L_1^{\Phi}(x_A - x_B)$, L_0^{Φ}, L_1^{Φ} are constants which have to be optimized.

Table 3.4. Expressions of Gibbs energies of pure components (including Cp)*.

No.	Gibbs Energy
1	$^{\circ}G_A^{\alpha} = 0$
2	$^{\circ}G_B^{\alpha} = 5009$
3	$^{\circ}G_A^{\gamma} = 23540 - 66.01T + [-0.275T^2 + 949.01T - 110Tln(T) - 73097\ ]$
4	$^{\circ}G_B^{\gamma} = 32690 - 80.12T + [-0.461T^2 + 1106T - 104Tln(T) - 119210] + [530]$
5	$^{\circ}G_A^{L} = 26291.4 - 73.25T + [-0.241T^2 + 714.68T - 80Tln(T).825 - 56507.82]$
6	$^{\circ}G_B^{\beta} = 0$

7	$^{\circ}G_A^{\beta} = 5200$
8	$^{\circ}G_B^{\gamma'} = 32690 - 80.12T + [-0.461T^2 + 1106T - 104Tln(T) - 119490.25]$
9	$^{\circ}G_A^{\gamma'} = 23540 - 66.01T + [-0.275T^2 + 949.01T - 110Tln(T) - 73097] + [600]$
10	$^{\circ}G_B^{L} = 36030 - 87.66T + [-0.4085T^2 + 730T - 57.714Tln(\mathrm{T}) - 88424.84]$

The terms in the first brackets represents the change due to the inclusion of C_P data and the second represents the estimate for the difference between the metastable and stable phases.

The optimization was carried out using the PARROT module of Thermo-Calc software. The optimized phase diagram for the AMPL-NPG system superimposed with DSC and X-ray diffraction data is shown in Figure 2. The expressing determined for the excess Gibbs energies are given below:

Table 3.5. Calculated Excess Gibbs energy Expressions

$G^{EX,\alpha} = x_A x_B\{1177\}$ $G^{EX,\beta} = x_A x_B\{1147 - 5.12(x_A - X_B)\}$

$G^{EX,\gamma} = x_A x_B\{4391 - 2.4(x_A - x_B)\ \}$ $G^{EX,\gamma} = x_A x_B\{5952 - 6.2(x_A - x_B)\}$

$G^{EX,L} = x_A x_B\{1600\}$

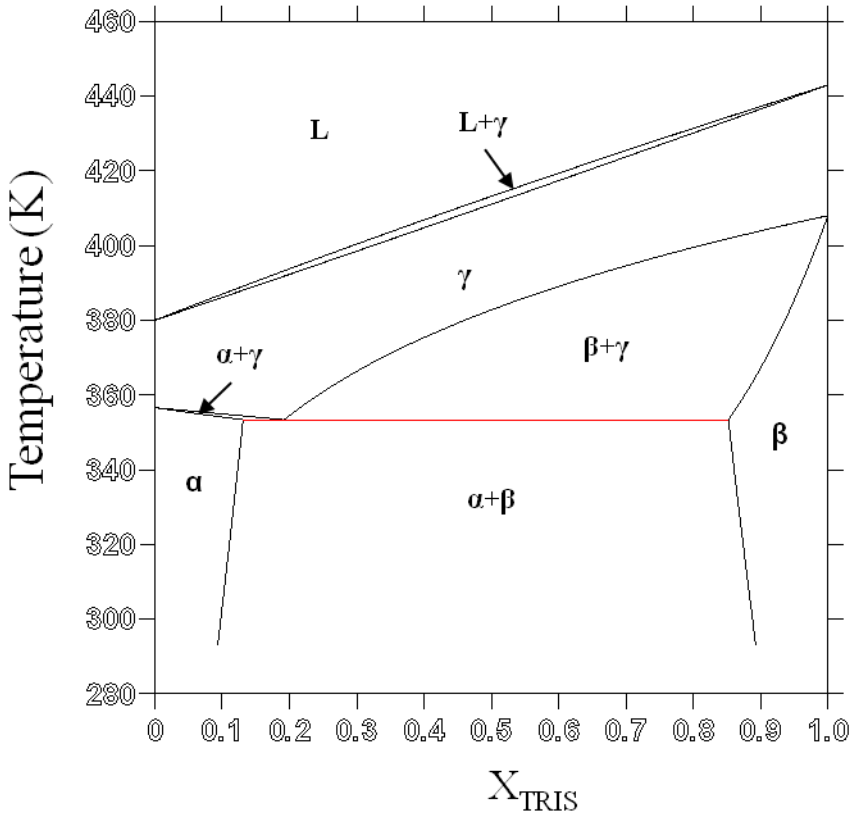

Fig 3.1. AMPL-TRIS without inclusion of Cp data; [Chandra et.al].

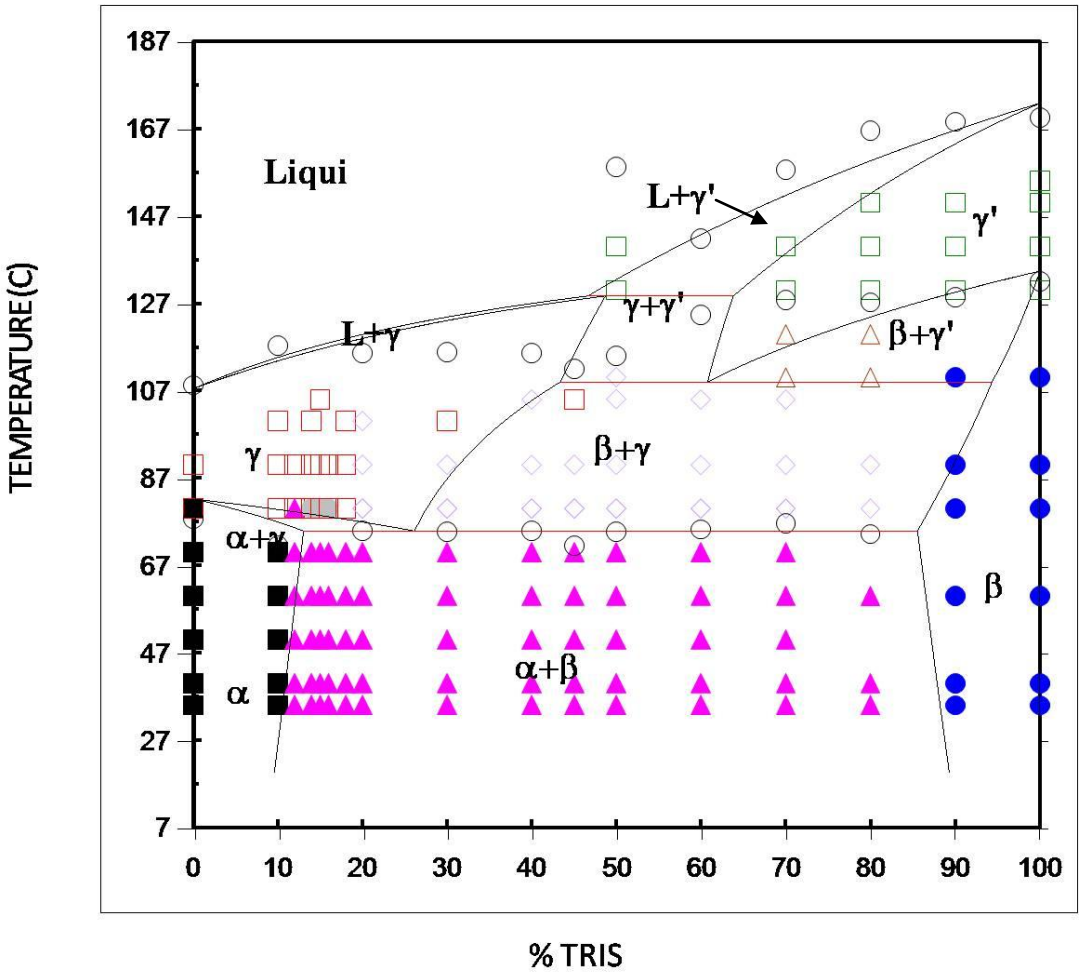

Fig 3.2. Unoptimized calculated diagram of TRIS-AMPL System with Cp data (Chandra et al [2] and V. Kamisetty [4]).

3.7. Optimization with L-terms

The optimization of the TRIS-AMPL is carried out by sub-regular solution model. The model solution is represented by the Redlich-Kister equations with L_0 and L_1 parameters to be optimized to give excess Gibbs energy of mixture between the plastic phases. The sub-regular model leads to a fair comparison of optimized fig 3 with the unoptimized fig-2. The Peritectic region at 401 K is extended for 5 to 10 K as shown in the optimized fig-3. The γ+γ' phase is observed between the temperatures 109 K and 128K which is appeared to be slightly shifted towards right when compared to the experimental data points. There is no good agreement with the experimental data in the L+γ region in this optimization.

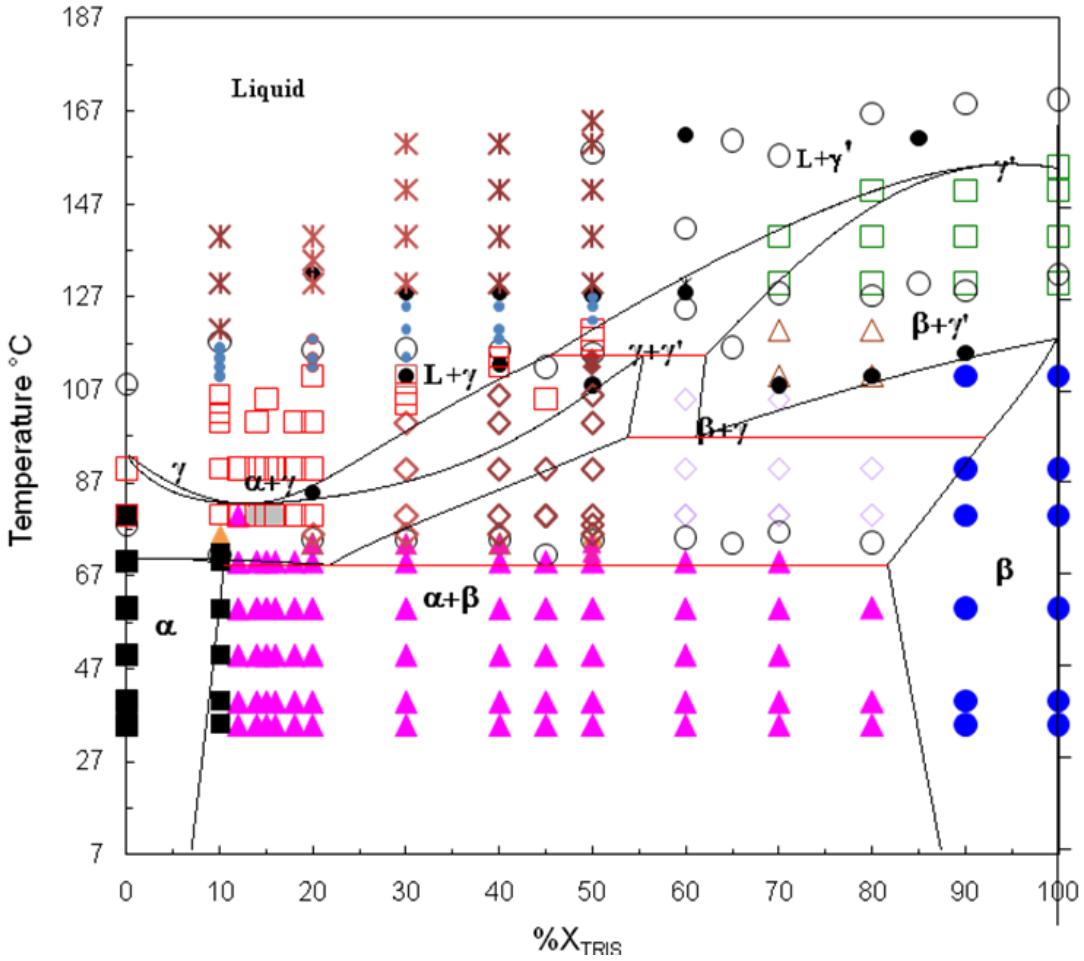

Fig 3.3. Optimized Phase Diagram of the TRIS-AMPL binary system superimposed with DSC and X-ray Diffraction data from Chandra et al [2] and V. Kamisetty [4].

Ideal solution behavior is assumed in estimating the metastable Gibbs energies of pure components. The ideal solution assumption is used only for metastable estimations and accounted for the non-ideality in high temperature γ' and γ phases by assuming sub-regular solution behavior, lower temperature (α and β) phases and the liquid phases are assumed to be ideal. Under ideal solution assumption for all the phases, the inclusion of heat capacity data to determine the Gibbs energies of various phases of pure components allowed better representation of the experimental invariant equilibria. The phase diagram without optimization did not showed the Peritectic phase transition at 401K and 49.7mol% TRIS however, and with incorporation it is closer to the experimental values.

The calculated TRIS-AMPL phase diagram in the earlier work [1] reproduced the global features of the experimental phase diagram but invariant equilibria temperatures between calculations and experiments differed by 5-7K, and also the fitting of invariant compositions was unsatisfactory. This calculation by [1] used the thermal analysis results and the results of crystallographic data stated that the miscibility is complete in the plastic phase and almost nonexistent in the ordered phases.

THERMO-CALC Files of Phase Diagram Calculations

TRIS-AMPL Phase Diagram - No Inclusion of Cp

LOGFILE GENERATED ON PC/WINDOWS NT DATE 2009-12-17

BY PRATHYUSHA

GO G

ENTER-ELEM A TR

AMEND-ELEM-DATA TR BE 70 -625800 -716.711

1

AMEND-ELEM-DATA A AL 50 -406000 -619.06

1

ENTER-PHASE AL,, 1 A TR; N N

ENTER-PHASE BE,, 1 TR A; N N

ENTER-PHASE GP,, 1 A TR; N N

ENTER-PHASE GA,, 1 TR A; N N

$ENTER-PHASE LIQ L 1 A TR; N N

ENTER-PHASE LIQ L 1 TR A; N N

ENTER-PARAMETER G(AL,A) 273.15 0; 550 N

ENTER-PARAMETER G(AL,TR) 273.15 5500; 550 N

ENTER-PARAMETER G(BE,TR) 273.15 0; 550 N

ENTER-PAR G(BE,A) 273.15 5200; 550 N

ENTER-PAR G(GA,A) 273.15 23540-66.01*T; 550 N

$23450-65.5*T

ENTER-PAR G(GA,TR) 273.15 32690-80.12*T; 550 N

ENTER-PAR G(GP,A) 273.15 23540-66.01*T; 550 N

ENTER-PAR G(GP,TR) 273.15 32690-80.12*T; 550 N

ENTER-PAR G(LIQ,A) 273.15 26291.4-73.25*T; 550 N

$26291.4-73.25*T

ENTER-PAR G(LIQ,TR) 273.15 36030-87.62*T; 550 N

ENTER-PAR L(AL,A,TR;0) 273.15 0; 550 N

ENTER-PAR L(AL,A,TR;1) 273.15 0; 550 N

ENTER-PAR L(BE,A,TR;0) 273.15 0; 550 N

ENTER-PAR L(BE,A,TR;1) 273.15 0; 550 N

ENTER-PAR L(GP,A,TR;0) 273.15 0; 550 N

ENTER-PAR L(GP,A,TR;1) 273.15 0; 550 N

ENTER-PAR L(LIQ,A,TR;0) 273.15 0; 550 N

ENTER-PAR L(GA,A,TR;0) 273.15 0; 550 N

ENTER-PAR L(GA,A,TR;1) 273.15 0; 550 N

```
GO POLY
DEF-COMP A TR
S-R-S A AL * 1E5
S-R-S A BE * 1E5
S-C N=1 T=340 P=1E5 X(TR)=0.18
C-E *
S-A-V 1 X(TR) 0 1 0.1
S-A-V 2 T 293 460 10
ADD,,,
SAVE TRIS-AMPL1 Y
MAP
PO
PLOT
SCREEN
SET-INTER
EXIT
```

TRIS-AMPL Phase Diagram - With Cp

LOGFILE GENERATED ON PC/WINDOWS NT DATE 2009-12-17

BY PRATHYUSHA

GO G

ENTER-ELEM A TR

AMEND-ELEM-DATA TR BE 70 -625800 -716.711

1

AMEND-ELEM-DATA A AL 50 -406000 -619.06

1

ENTER-PHASE AL,, 1 A TR; N N

ENTER-PHASE BE,, 1 TR A; N N

ENTER-PHASE GP,, 1 A TR; N N

ENTER-PHASE GA,, 1 TR A; N N

$ENTER-PHASE LIQ L 1 A TR; N N

ENTER-PHASE LIQ L 1 TR A; N N

ENTER-PARAMETER G(AL,A) 273.15 0; 550 N

ENTER-PARAMETER G(AL,TR) 273.15 5500; 550 N

ENTER-PARAMETER G(BE,TR) 273.15 0; 550 N

ENTER-PAR G(BE,A) 273.15 5200; 550 N

ENTER-PAR G(GA,A) 273.15 23450-65.5*T-0.275*T**2

+949.01*T-110*T*LN(T)-73097.475+2035.3-800-70; 550 N

ENTER-PAR G(GA,TR) 273.15 32690-80.12*T-0.45*T**2

+1106*T-104*T*LN(T)-119210.25-1820-230; 550 N

ENTER-PAR G(GP,A) 273.15 23450-65.5*T-0.275*T**2

+949.01*T-110*T*LN(T)-73097.475; 550 N

ENTER-PAR G(GP,TR) 273.15 32690-80.12*T-0.461*T**2

+1106*T-104*T*LN(T)-119210.25+2125-1320-150; 550 N

ENTER-PAR G(LIQ,A) 273.15 26291.4-73.25*T-0.241*T**2

+714.68*T-80*T*LN(T)-56507.825-60; 550 N

ENTER-PAR G(LIQ,TR) 273.15 36030-87.4*T-0.411*T**2

+730*T-57.714*T*LN(T)-88174.84+850-50; 550 N

ENTER-PAR L(AL,A,TR;0) 273.15 0; 550 N

ENTER-PAR L(AL,A,TR;1) 273.15 0; 550 N

ENTER-PAR L(BE,A,TR;0) 273.15 0; 550 N

ENTER-PAR L(BE,A,TR;1) 273.15 0; 550 N

ENTER-PAR L(GP,A,TR;0) 273.15 0; 550 N

ENTER-PAR L(GP,A,TR;1) 273.15 0; 550 N

```
ENTER-PAR L(LIQ,A,TR;0) 273.15 0; 550 N
ENTER-PAR L(GA,A,TR;0) 273.15 0; 550 N
ENTER-PAR L(GA,A,TR;1) 273.15 0; 550 N

GO POLY
DEF-COMP A TR
S-R-S A AL * 1E5
S-R-S A BE * 1E5
S-C N=1 T=340 P=1E5 X(TR)=0.18
C-E *
S-A-V 1 X(TR) 0 1 0.1
S-A-V 2 T 293 453 10
ADD,,,
SAVE TRIS-AMPL1 Y
MAP
PO
PLOT
SCREEN
SET-INTER
EXIT
```

TRIS-AMPL Phase Diagram - FINAL OPTIMIZATION

LOGFILE GENERATED ON PC/WINDOWS NT DATE 2009-12-17

BY PRATHYUSHA

GO G

ENTER-ELEM A TR

AMEND-ELEM-DATA TR BE 70 -625800 -716.711

1

AMEND-ELEM-DATA A AL 50 -406000 -619.06

1

ENTER-PHASE AL,, 1 A TR; N N

ENTER-PHASE BE,, 1 TR A; N N

ENTER-PHASE GA,, 1 A TR; N N

ENTER-PHASE GP,, 1 TR A; N N

$ENTER-PHASE LIQ L 1 A TR; N N

ENTER-PHASE LIQ L 1 TR A; N N

ENTER-PARAMETER G(AL,A) 273.15 0; 550 N

ENTER-PARAMETER G(AL,TR) 273.15 5009; 550 N

ENTER-PARAMETER G(BE,TR) 273.15 0; 550 N

ENTER-PAR G(BE,A) 273.15 5173; 550 N

ENTER-PAR G(GA,A) 273.15 23540-66.01*T-0.275*T**2
+949.461*T-110*T*LN(T)-73097.475; 550 N

ENTER-PAR G(GA,TR) 273.15 32690-80.12*T-0.461*T**2
+1106*T-104.09*T*LN(T)-119210.25+530; 550 N

ENTER-PAR G(GP,A) 273.15 23540-66.01*T-0.275*T**2
+949.01*T-110*T*LN(T)-73097.475+600; 550 N

ENTER-PAR G(GP,TR) 273.15 32690-80.12*T-0.461*T**2
+1106*T-104.09*T*LN(T)-119490.25; 550 N

ENTER-PAR G(LIQ,A) 273.15 26291.4-73.25*T-0.241*T**2
+714.68*T-80*T*LN(T)-56507.825; 550 N

ENTER-PAR G(LIQ,TR) 273.15 36030-87.66*T-0.4085*T**2
+730*T-57.714*T*LN(T)-88424.84; 550 N

ENTER-PAR L(AL,A,TR;0) 273.15 1177; 550 N

ENTER-PAR L(BE,A,TR;0) 273.15 1147-5.12*T; 550 N

ENTER-PAR L(GA,A,TR;0) 273.15 1720-2.3*T ; 550 N

ENTER-PAR L(GA,A,TR;1) 273.15 2671-0.1*T; 550 N

ENTER-PAR L(LIQ,TR,A;0) 273.15 1600; 550 N

ENTER-PAR L(GP,A,TR;0) 273.15 1827+0.05*T; 550 N

ENTER-PAR L(GP,A,TR;1) 273.15 4125-6.7*T; 550 N

GO POLY

DEF-COMP A TR

S-R-S A AL * 1E5

S-R-S A BE * 1E5

S-C N=1 T=340 P=1E5 X(TR)=0.18

C-E *

S-A-V 1 X(TR) 0 1 0.1

S-A-V 2 T 293 453 20

ADD,,,

SAVE TRIS-AMPL1 Y

MAP

PO

S-D-A

Y

T-C

PLOT

SCREEN

SET-INTER

EXIT

== OPTIMIZING VARIABLES ==

AVAILABLE VARIABLES ARE V1 TO V00

VAR.	VALUE	START VALUE	SCALING FACTOR	REL.STAND.DEV
V11	1.17700000E+03			
V21	1.14700000E+03			
V22	-5.12153615E+00			
V31	1.72013028E+03			
V32	-2.31980977E+00			
V33	2.67100000E+03			
V34	-1.00000000E-01			
V41	1.82734626E+03			
V42	5.00000000E-02			
V43	4.12554034E+03			
V44	-6.70000000E+00			
V51	1.60000000E+03			

NUMBER OF OPTIMIZING VARIABLES: 1

ALL OTHER VARIABLES ARE FIX WITH THE VALUE ZERO

3.8. Conclusions

The phase diagram for the TRIS-AMPL system has been calculated utilizing a simple estimation for metastable Gibbs energies, in combination with thermodynamic optimization. The experimental data for the thermodynamic properties has been considered during the optimization. It can be seen that there is a good agreement with the calculated results and the experimental data of V. Kamisetty. The low-temperature α and β phases and the liquid phase were assumed to be ideal. An initial assumption of ideality in the high-temperature phases is used only to estimate the metastable Gibbs energies. The non-ideality of the solution phases for γ and γ' have been modeled as sub-regular solutions. The optimization using Thermo-Calc software included data only from the phase diagram (tie line, invariant equilibria composition and temperatures). There is good agreement between the calculated and experimental phase boundaries and invariant equilibria. The agreement between the calculated and measured values of the enthalpies of fusion is not very good but reasonable especially since the measured values were not used in the thermodynamic optimization.

The magnitude of heat capacities (~32^{o}C to 177 ^{o}C) for these organic Plastic Crystals is relatively high and they result from sharp increases during the solid-solid phase transitions. Such changes become significant since they also have low melting temperatures (~77 ^{o}C to 167 ^{o}C). These effects can become important when making an initial phase diagram calculation in the absence of any experimental phase diagram data and help us narrow down the expected phase diagram behavior.

3.9. References

[1] M. Barrio, J. Font, J. Chem. Phys., 91 (1994), 189-202.

[2] D. Chandra, Suresh Divi, Raja Chellappa, J. Chem. Thermodynamics 38 (2006) 1312-1326.

[3] R. Chellappa, Phase Diagram Calculations and High Pressure Raman Spectroscopy Studies of Organic 'Plastic Crystal' Thermal Energy Storage Materials, Ph.D Dissertation, University of Nevada, Reno, 2005.

[4] V. Kamisetty, Pressure-Temperature Phase Diagram of Tris (Hydroxymethyl) Aminomethane and Phase Diagram Determination of Tris (Hydroxymethyl) Aminomethane − 2-Amino-2-Methyl-1, 3-Propanediol (AMPL) Binary System MS Thesis, University of Nevada, Reno, 2010.

[5] Robert T. DeHoff, Thermodynamics in Materials, (2002).